RSC Medicinal Chemistry

ROYAL SOCIETY OF CHEMISTRY

RESEARCH ARTICLE

View Article Online
View Journal | View Issue

Cite this: *RSC Med. Chem.*, 2025, **16**, 5472

Targeting tumor-associated hypoxia with bioreductively activatable prodrug conjugates derived from dihydronaphthalene, benzosuberene, and indole-based inhibitors of tubulin polymerization

Zhe Shi, [a] Rajsekhar Guddneppanavar,[a] Blake A. Winn,[a] Matthew T. MacDonough,[a] Clinton S. George,[a] Yifan Wang,[a] Mark Zimmer,[a] Jeni Gerberich,[b] Alex Winters,[b] Elisa Lin,[b] Casey J. Maguire,[a] Jacob Ford,[a] Ernest Hamel, [c] Ralph P. Mason, [b] Mary Lynn Trawick[a] and Kevin G. Pinney *[a]

A strategy for targeting tumor-associated hypoxia utilizes reductase enzyme-mediated cleavage to convert biologically inert prodrugs to their corresponding biologically active parent therapeutic agents selectively in areas of pronounced hypoxia. Small-molecule inhibitors of tubulin polymerization represent unique therapeutic agents for this approach, with the most promising functioning as both antiproliferative agents (cytotoxins) and as vascular disrupting agents (VDAs). VDAs selectively and effectively disrupt tumor-associated microvessels, which are typically fragile and chaotic in nature. VDA treatment may augment existing tumor-associated hypoxia, thus enhancing the efficacy of hypoxia-selective prodrugs. Structure activity relationship-guided studies in our laboratories led to the discovery of promising lead molecules (OXi6196, KGP05, KGP18, and OXi8006) that bind to the colchicine site on the tubulin heterodimer. A series of bioreductively activatable prodrug conjugates (BAPCs) based on these molecules was synthesized utilizing ether-linked heteroaromatic hypoxia-selective triggers bearing a nitro group. Biological evaluation against the A549 human lung carcinoma cell line (under normoxic *versus* anoxic conditions) revealed several BAPCs with positive hypoxia cytotoxicity ratios. Preliminary *in vivo* evaluation of a representative BAPC (**KGP291**) demonstrated vascular shutdown in nude mice bearing orthotopic 4T1 breast tumors studied by bioluminescence imaging.

Received 25th June 2025,
Accepted 15th August 2025

DOI: 10.1039/d5md00564g

rsc.li/medchem

1. Introduction

Tumor-associated hypoxia[1] results, in part, from the disproportional distribution of blood vessels throughout tumor tissue, which is further augmented by the fragile and chaotic nature of these microvessels.[2] The resulting regions of low oxygen concentration promote angiogenic signaling and increase metastatic potential. Tumor microcirculation and oxygenation play critical roles in tumor growth, affecting drug delivery, metastatic spread, and responsiveness to cytotoxic chemotherapy and therapeutic irradiation.[3] Studies have shown poor prognosis and increased metastasis for patients with hypoxic tumors with respect to diverse therapies.[4] While tumor-associated hypoxia is associated with an array of challenges in the treatment of cancer, it also presents opportunities for selective drug delivery through appropriate hypoxia-selective prodrug strategies.[5–11] Most solid tumors contain hypoxic regions, and certain reductase enzymes (such as NADPH cytochrome P450 reductase) are capable of irreversibly reducing a variety of substrates under the hypoxic conditions of these tumors.[12–17]

A variety of chemical entities (triggers) are susceptible to one- or two-electron reductase enzymes, which mediate reduction of the trigger and subsequent release of the parent therapeutic agent. Commonly employed triggers include nitro-heterocycles, aromatic *N*-oxides, aliphatic *N*-oxides, quinones, and metal complexes.[26–31] Several bioreductive prodrugs have undergone clinical evaluation (Fig. 1),[18] including evofosfamide (TH-302),[10,19] apaziquone

[a] *Department of Chemistry and Biochemistry, Baylor University, One Bear Place #97348, Waco, TX 76798-7348, USA. E-mail: Kevin_Pinney@baylor.edu; Tel: +1 254 710 4117*
[b] *Prognostic Imaging Research Laboratory, Department of Radiology, University of Texas Southwestern Medical Center, 5323 Harry Hines Boulevard, Dallas, TX 75390, USA*
[c] *Molecular Pharmacology Branch, Developmental Therapeutics Program, Division of Cancer Treatment and Diagnosis, National Cancer Institute, Frederick National Laboratory for Cancer Research, National Institutes of Health, Frederick, MD 21702, USA*

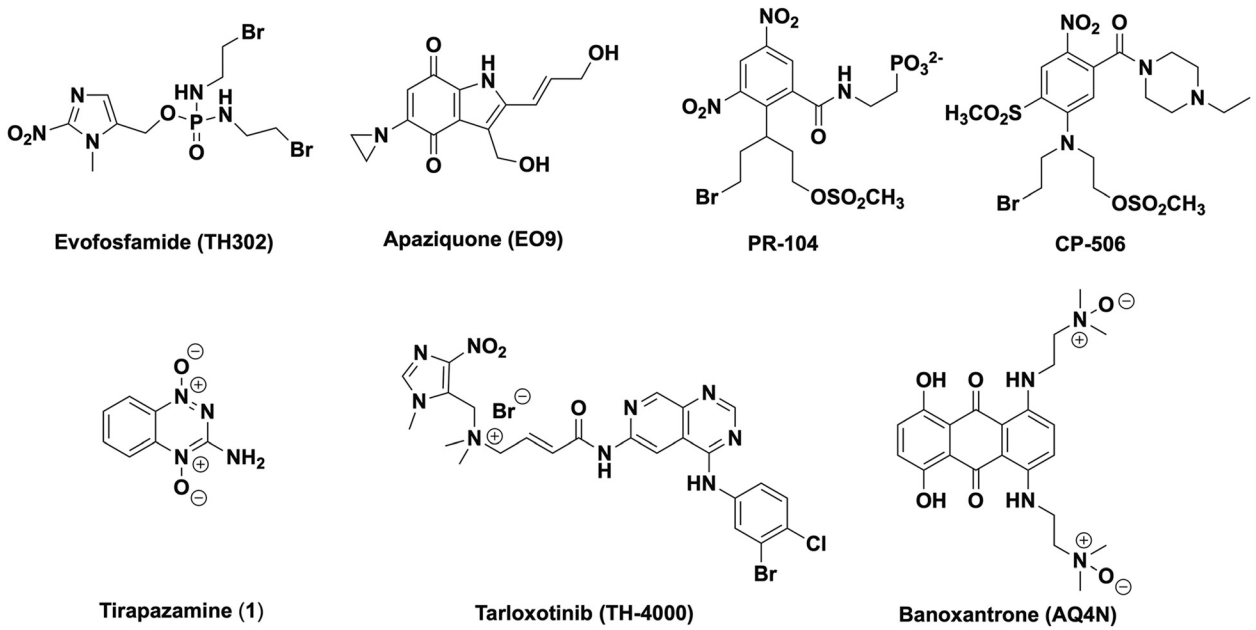

Fig. 1 Representative hypoxia-activated prodrugs evaluated previously in the clinic.[10,18–25]

(EO9),[20] PR-104,[21] tirapazamine,[22,23] tarloxotinib (TH-4000),[18] CP-506,[24] and banoxantrone (AQ4N).[25] Despite significant research efforts in the area of hypoxia targeted cancer therapies, no such agent, to date, has received approval from the United States Food and Drug Administration (FDA). This lack of clinical progress has been attributed in part to the difficulty of selecting patients who have very hypoxic tumors. Efforts are underway to identify tumors in patients that are characterized by molecular features, such as strong hypoxia gene expression signature, indicating potential for treatment benefit.[7,32]

Bioreductively activatable prodrug conjugates (BAPCs) are designed to be biologically inert under aerobic conditions, but under hypoxic conditions enzyme-mediated reduction results in cleavage of the prodrug construct to release the active therapeutic agent. Judicious combination of an appropriate trigger (to facilitate hypoxia-selective release) coupled to a promising therapeutic agent is deemed paramount for success. A foundational study by Davis and co-workers utilized the natural product combretastatin A-4 (CA4) as a tubulin-binding agent in a series of synthesized BAPCs.[43] CA4 is a potent inhibitor of tubulin assembly that demonstrates low nM cytotoxicity against a wide variety of human cancer cell lines.[33] Drawing structural inspiration, in part, from CA4, our previous studies led to the design and synthesis of a variety of small-molecule inhibitors of tubulin polymerization. Representative examples (Fig. 2) include dihydronaphthalene, benzosuberene,

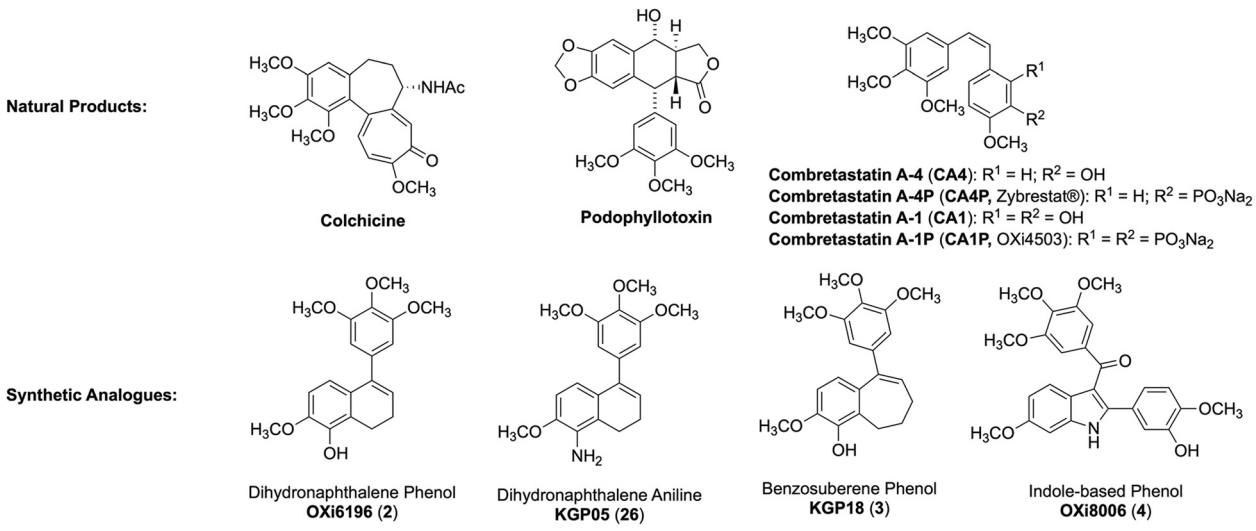

Fig. 2 Representative small-molecule inhibitors of tubulin polymerization.[33–42]

and indole-based analogues.[35–39,44–48] Furthermore, CA4 functions as a vascular disrupting agent (VDA),[49,50] facilitating effective and selective shutdown of blood flow to tumors. While the endothelium of normal blood vessels is remodeled and largely quiescent, the neovasculature of tumors is primitive, more responsive to angiogenic cell signaling, and activated in nature.[51] Consequently, the tumor vasculature offers an excellent, selective target for anticancer therapy. The goal of VDAs is to cause rapid and widespread disruption of existing tumor vasculature leading to blood flow shutdown to the tumor followed by massive tumor necrosis.[51,52] This mechanism is distinct from that of angiogenesis inhibiting agents (AIAs), which prevent the growth of new blood vessels.[51] Davis and co-workers prepared a series of CA4-BAPCs (Fig. 3) that utilized ether-linked nitrothienyl bioreductive triggers.[43] These CA4-based BAPCs demonstrated selective release of CA4 under hypoxic conditions. Guided by these results (Fig. 3), we previously synthesized and evaluated for biological activity a series of phenstatin-BAPCs[53,54] and separately a series of BAPCs based on the natural product combretastatin A-1 (CA1).[55]

A long-standing program in the design, synthesis, and biological evaluation of small-molecule inhibitors of tubulin polymerization resulted in our discovery and development of a wide-variety of molecules, including dihydronaphthalene, benzosuberene and indole analogues inspired, in part, by colchicine and CA4.[35–39,56–58] A subset of these molecules demonstrated dual efficacy by functioning biologically as both potent antiproliferative agents (cytotoxins) and as promising VDAs. There are a variety of potential benefits of these dihydronaphthalene, benzosuberene, and indole analogues in comparison to CA4, including enhanced stability due to replacement of the *Z*-ethylene bridge of CA4 with fused cyclic ring systems. Utilizing the corresponding phenolic-based analogues (OXi6196, KGP18, and OXi8006), along with an aniline-based analogue (KGP05) as the small-molecule parent therapeutic agents (Fig. 2), a series of BAPCs bearing nitrothiophene, nitroimidazole, and nitrofuran bioreductive triggers were synthesized. These BAPCs were designed to undergo reductase-mediated cleavage (Fig. 4) under hypoxic conditions. This type of cleavage is most likely facilitated by the activity of NADPH cytochrome P450 oxidoreductase and may proceed *via* the initially generated radical anion as suggested by pulse radiolysis studies by Davis and co-workers with a CA4-BAPC.[43] Alternatively, further reduction of the radical anion to the corresponding hydroxy amine or amine may then proceed to release the parent therapeutic agent *via* a cascade fragmentation sequence.

2. Results and discussion

2.1. Synthesis

The synthesis of dihydronaphthalene-BAPCs (**12–18**) and benzosuberene-BAPCs (**19–22**) was accomplished using Mitsunobu conditions (Scheme 1), a strategy previously employed to generate CA4-BAPCs, phenstatin-BAPCs, and CA1-BAPCs, along with other hypoxia-activated prodrugs.[43,54,55,59,60] The potent tubulin binding agents (**OXi6196**, **KGP18**, **OXi8006**) utilized in this study were prepared as previously described.[35–38,45,47,61] The bioreductive triggers (**5–11**) were synthesized utilizing previously reported procedures.[54,59] Coupling of the tubulin binding therapeutic small-molecule with the requisite bioreductive trigger was accomplished using Mitsunobu reaction conditions to generate the ether linkage.[43,54,55,62] Indole-BAPCs (**23–25**) were synthesized in the same manner. **OXi8006** (**4**) and nitrothiophene triggers (**5–7**) were coupled through an ether linkage using Mitsunobu conditions (Scheme 2). Diisopropyl azodicarboxylate (DIAD) and triphenylphosphine were suitable Mitsunobu partners for the *nor*- and *mono*-methyl OXi8006-nitrothiophene BAPCs (**23–24**). However, the use of 1,1′-(azodicarbonyl)dipiperidine (ADDP) and tributylphosphine proved necessary for successful synthesis of the *gem*-dimethyl OXi8006-nitrothiophene BAPC (**25**). While indole-based BAPCs **23** and **24** were obtained with relatively high purity, the indole *gem*-dimethyl analogue **25** only reached a purity level of 74% after purification. Importantly, HPLC indicated that no OXi8006 was present as an impurity. A series of nitrofuran-based and carbamate- or carbonate-based BAPCs were also synthesized (see SI). It should be noted that molecules

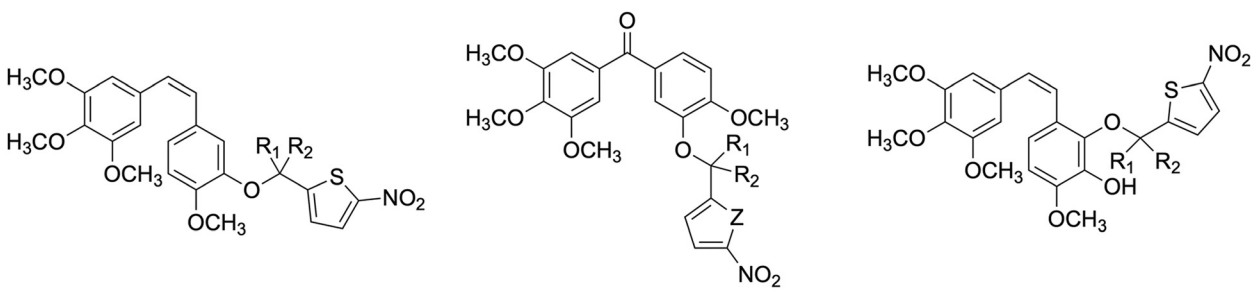

Fig. 3 Representative previously reported BAPCs that incorporate tubulin binding therapeutic agents.[43,54,55]

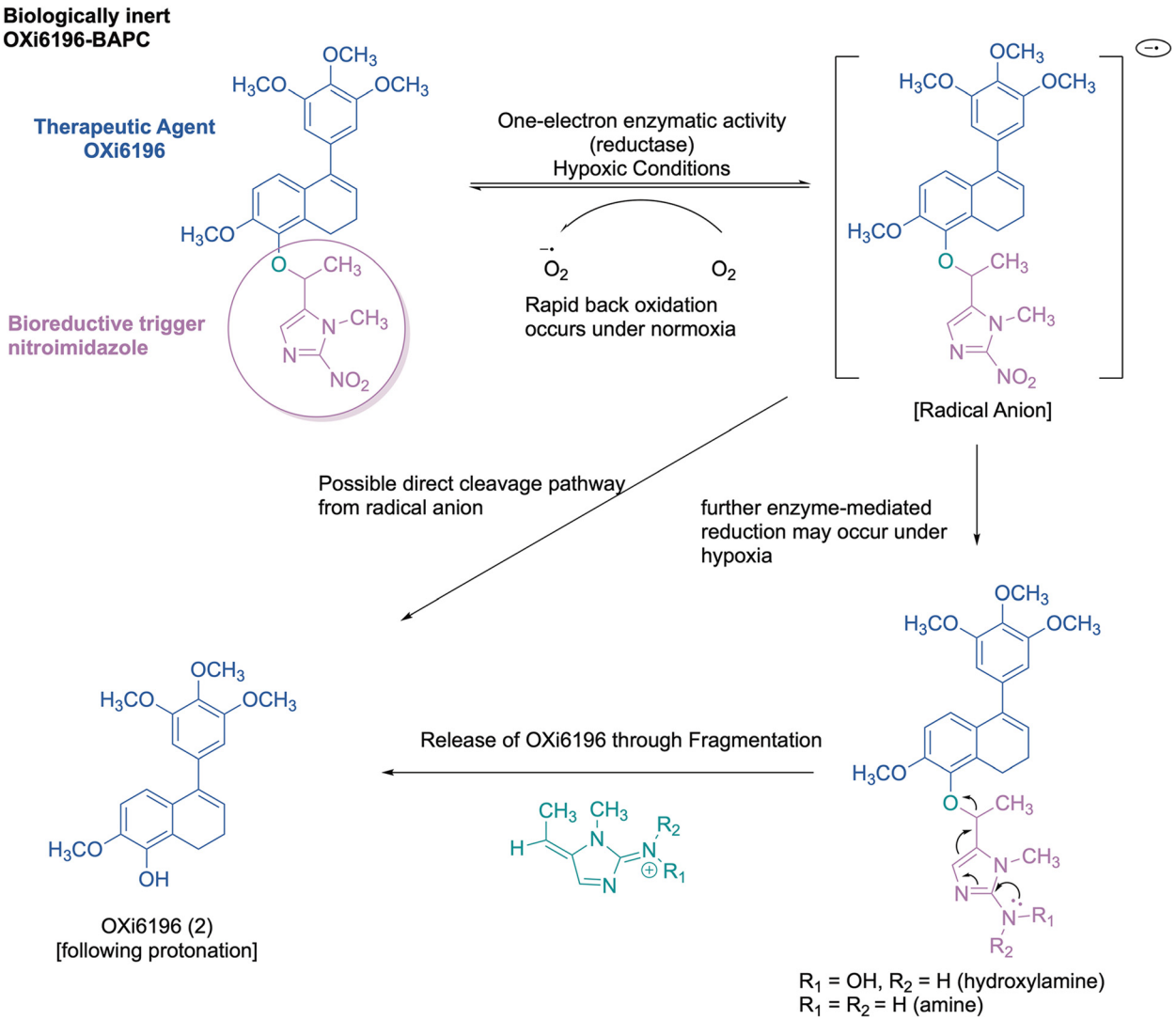

Fig. 4 Hypoxia-facilitated, enzyme-mediated reduction and cleavage of BAPCs (OXi6196-BAPC as a representative example).

containing a stereogenic center were synthesized and biologically evaluated as racemic mixtures. While there are potential toxicity concerns related to the incorporation of nitroaryl moieties in therapeutic agents,[63] there are also many benefits leading to unique pharmacophore-driven bioactivity against diverse targets.[64] Future studies will be necessary to evaluate the PK, ADME, and toxicology profiles associated with the BAPCs in this study, but a significant number of drugs containing a nitroaryl moiety have received FDA approval.[64]

2.2. Biological evaluation

BAPCs and corresponding parent therapeutic agents (**OXi6196**, **KGP18**, and **OXi8006**) were evaluated for their ability to inhibit tubulin assembly and colchicine binding. BAPCs were all found to be inactive (IC_{50} > 20 μM) as inhibitors of tubulin assembly as anticipated (Table S1). This confirmed that attachment of the bioreductive trigger dramatically inhibited binding to the colchicine site by the BAPC. Cytotoxicity under both normoxic and hypoxic conditions was evaluated in the A549 cell line (human lung carcinoma) to observe differential growth inhibition of the A549 cells. Prior studies by us and others demonstrated the feasibility of using A549 cells under hypoxic *versus* normoxic conditions to facilitate activation of hypoxia-selective prodrugs and probes bearing nitroaryl triggers, and separately tirapazamine.[22,43,54,55,65] In addition, lung tumors have been characterized with distinct regions of hypoxia.[66] Two distinct protocols were utilized to evaluate the different BAPCs against the A549 cells under both normoxic and hypoxic conditions. In one protocol (Table 1 data), plates were incubated for 4 h under anaerobic conditions to trigger prodrug cleavage, followed by a 48 h incubation under aerobic conditions without changing the media, in order to assess antimitotic effects. In a second protocol (Table S3), plates were incubated for 4 h under anaerobic conditions followed by 120 h under aerobic conditions after removal of media containing drug (and replacement of media), prior to determination of cytotoxicity by the sulforhodamine B (SRB) assay. Several BAPCs in the

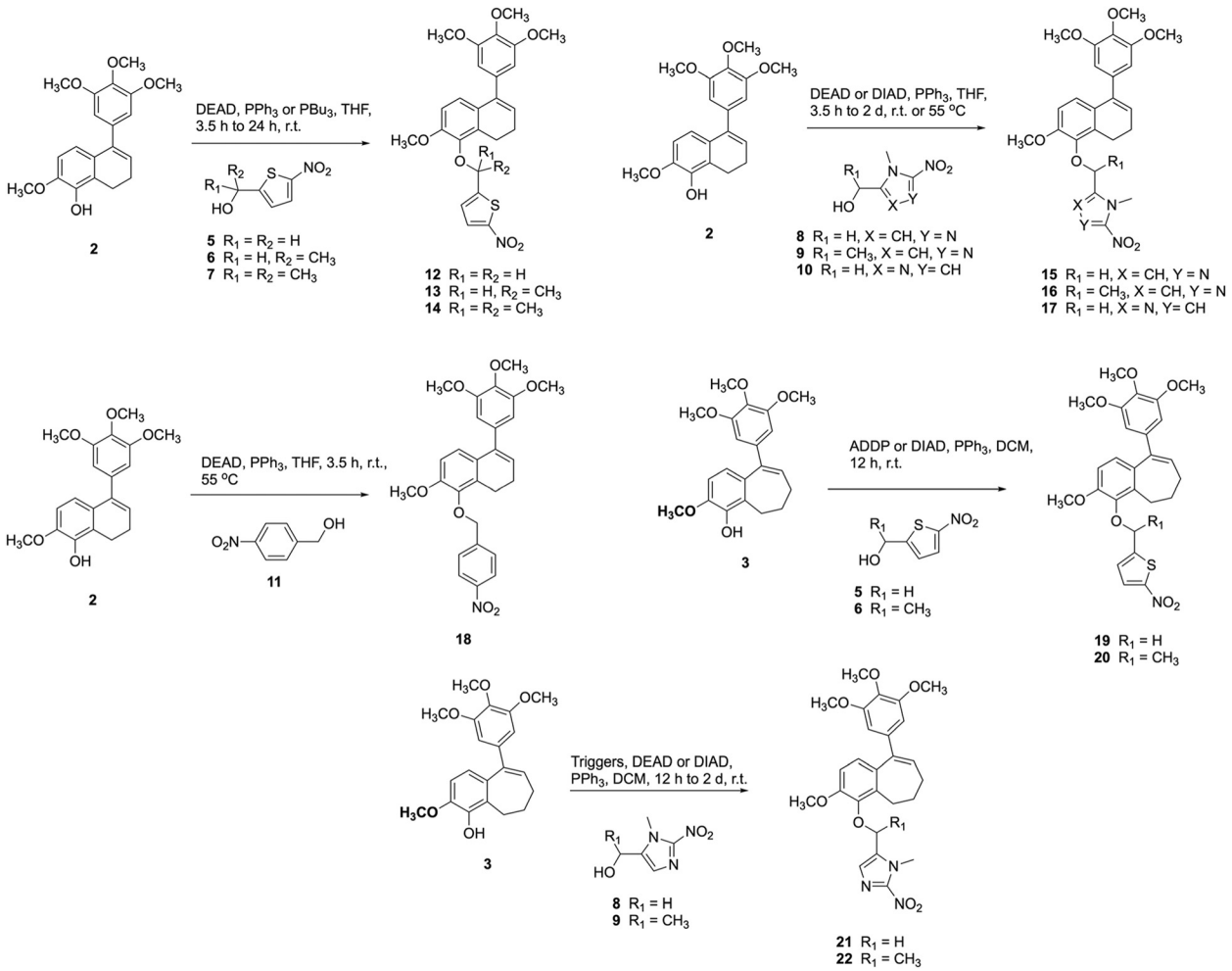

Scheme 1 Synthetic routes toward **OXi6196** and **KGP18**-BAPCs (**12**–**22**).

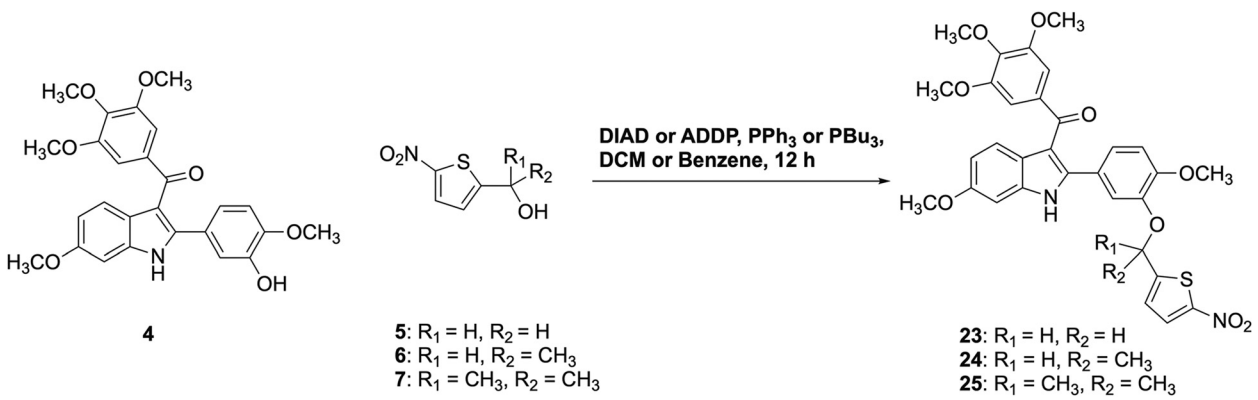

Scheme 2 Synthetic routes toward **OXi8006**-BAPCs (**23**–**25**).

dihydronaphthalene and benzosuberene series (**13**–**16**, **20**–**22**) demonstrated enhanced cytotoxicity (see Table 1) under hypoxic conditions and BAPCs **13**, **16**, and **21** displayed hypoxic cytotoxicity ratios (HCRs) > 7.5, comparable to that of tirapazamine (HCR = 8.9), used as a positive control. The indole series of BAPCs (**23**–**25**) were exemplary with HCR values ranging from 33.8 for BAPC **24** to 79 for BAPC **25** and 79.7 for BAPC **23** (Table 1). HCR values for tirapazamine (TPZ) were consistently lower in this assay compared to the second protocol in which the drug was removed after 4 h of incubation under anaerobic conditions (HCR ≫ 32). In a separate study with BAPC removal after 48 h and longer (120 h) aerobic exposure

Table 1 *In vitro* potency and hypoxia cytotoxicity ratio (HCR) in A549 human cancer cell line

Compound	IC_{50} [oxic] (μM) ± SEM[a,b]	IC_{50} [anoxic] (μM) ± SEM[a,b]	HCR
TPZ (**1**)	63.5	7.1	8.9
OXi6196 (**2**)	0.0066[c]	ND[d]	ND[d]
KGP18 (**3**)	0.000027[c]	ND[d]	ND[d]
OXi8006 (**4**)	0.030[c]	ND[d]	ND[d]
KGP24 (**12**)	0.46 ± 0.05	0.48 ± 0.04	1.0
KGP25 (**13**)	2.74 ± 1.13	0.25 ± 0.08	11.0
KGP66 (**14**)	0.13 ± 0.06	0.05 ± 0.01	2.6
KGP105 (**15**)	0.25 ± 0.02	0.04 ± 0.003	6.2
KGP291 (**16**)	0.38 ± 0.03	0.05 ± 0.004	7.6
KGP30 (**17**)[e]	ND[d]	ND[d]	ND[d]
KGP29 (**18**)[e]	ND[d]	ND[d]	ND[d]
KGP305 (**19**)	0.05 ± 0.005	0.22 ± 0.09	0.2
KGP304 (**20**)	2.27 ± 1.01	0.38 ± 0.12	6.0
KGP293 (**21**)	0.36 ± 0.02	0.04 ± 0.005	9.0
KGP292 (**22**)	0.67 ± 0.13	0.14 ± 0.04	4.8
KGP311 (**23**)	5.58 ± 3.59	0.07 ± 0.04	79.7
KGP343 (**24**)	4.06 ± 1.89	0.12 ± 0.06	33.8
KGP354 (**25**)	5.53 ± 2.22	0.07 ± 0.02	79

[a] Average of $n \geq 3$ independent determinations. [b] 4 h incubation (oxic or anoxic) followed by 48 h oxic exposure. [c] Values for standard SRB assay for cytotoxicity in A549 cells. [d] ND = not determined. [e] See Table S3 for HCR data under different assay conditions.

time (Table S3), BAPC **17** demonstrated an HCR = 14, while several other BAPCs returned positive HCR values ranging from 4.8 to 0.8 (see Table S3). Positive controls under this assay protocol included TPZ (HCR ≫ 32) and RB6145 (HCR > 3). RB6145 is a nitroimidazole-based bifunctional radiosensitizer prodrug.[67] It should be noted that due, in part, to historical sequencing of assay conditions utilized in our laboratory, not all BAPCs were evaluated for HCR determination under both assay protocols.

Representative BAPCs were evaluated for their stability (phosphate buffer, pH 7.4) and their ability to undergo enzymatic cleavage by NADPH cytochrome P450 oxidoreductase (POR), an enzyme implicated in the bioreductive activation of a number of prodrugs,[68,69] in a cell-free assay (Table S4). While positive HCR values correlated, in general, with observed enzyme-mediated cleavage (to release the parent therapeutic agent), the observed cleavage was often fairly low, except in the case of BAPC **14** (98% cleavage) and BAPC **25** (100% cleavage). In general, the BAPCs evaluated showed excellent stability in phosphate buffer.

Preliminary *in vivo* evaluation of BAPC KGP291 (16) as a hypoxia activated VDA. The dynamic and longitudinal effects of a BAPC being activated to release its linked therapeutic agent, which functions as both a cytotoxin and VDA, can be assessed with various non-invasive imaging modalities.[70] Bioluminescence imaging (BLI) is a widely used optical technique for preclinical research.[70–72] The light emission of BLI is based on the expression of the luciferase enzyme and the presence of the substrate luciferin. The effect of VDAs can be observed through reduced delivery of the substrate luciferin, due to VDA-induced damage to tumor-associated microvessels, and consequent diminished light emission, as has been demonstrated with several VDAs.[70,73–75] It is noteworthy that our prior research with various mouse models of cancer involving the parent therapeutic agents utilized in this study, including OXi6196 (parent agent of BAPC KGP291), provided pertinent guidance on initial dose selection for the *in vivo* study.[73–75] We performed a preliminary dose escalation study on three nude mice with 4T1-luc tumors[76] with respective doses of 29, 53, or 61 mg kg^{-1} **KGP291** administered intraperitoneally. Two additional mice served as controls, with one treated with vehicle (10% DMSO : 90% sesame oil) and the other treated with single dose **OXi6197** (30 mg kg^{-1}), the phosphate salt prodrug of compound **2**. Tumors treated with single dose **KGP291** (61 mg kg^{-1}) and **OXi6197** showed dramatic vascular shutdown within 4 h, evidenced by substantial reduction in the BLI signal at 4 and 24 h after administration of each compound (Fig. 5 and 6). These results provide preliminary evidence that KGP291 underwent *in vivo* reductase enzyme-mediated cleavage to release parent agent OXi6196 in the tumor microenvironment, leading to tumor-associated microvessel damage. This damage was initially observed at 4 h and was sustained at 24 h for mice receiving the higher doses (53 and 61 mg kg^{-1}) as fresh injections of luciferin at each of those time points resulted in diminished BLI signal compared to control. The effect was most evident in the mouse receiving 61 mg kg^{-1} of KGP291. All animal experiments and procedures were carried out in accordance with the State of Texas and United States (US) Federal guidelines and were approved by the Institutional Animal Care and Use Committee (IACUC) of the University of Texas Southwestern Medical Center under APN101222 and APN102169.

3. Conclusion

In this study, potent colchicine binding site inhibitors and VDAs (**OXi6196**, **KGP18**, and **OXi8006**) were coupled to a series

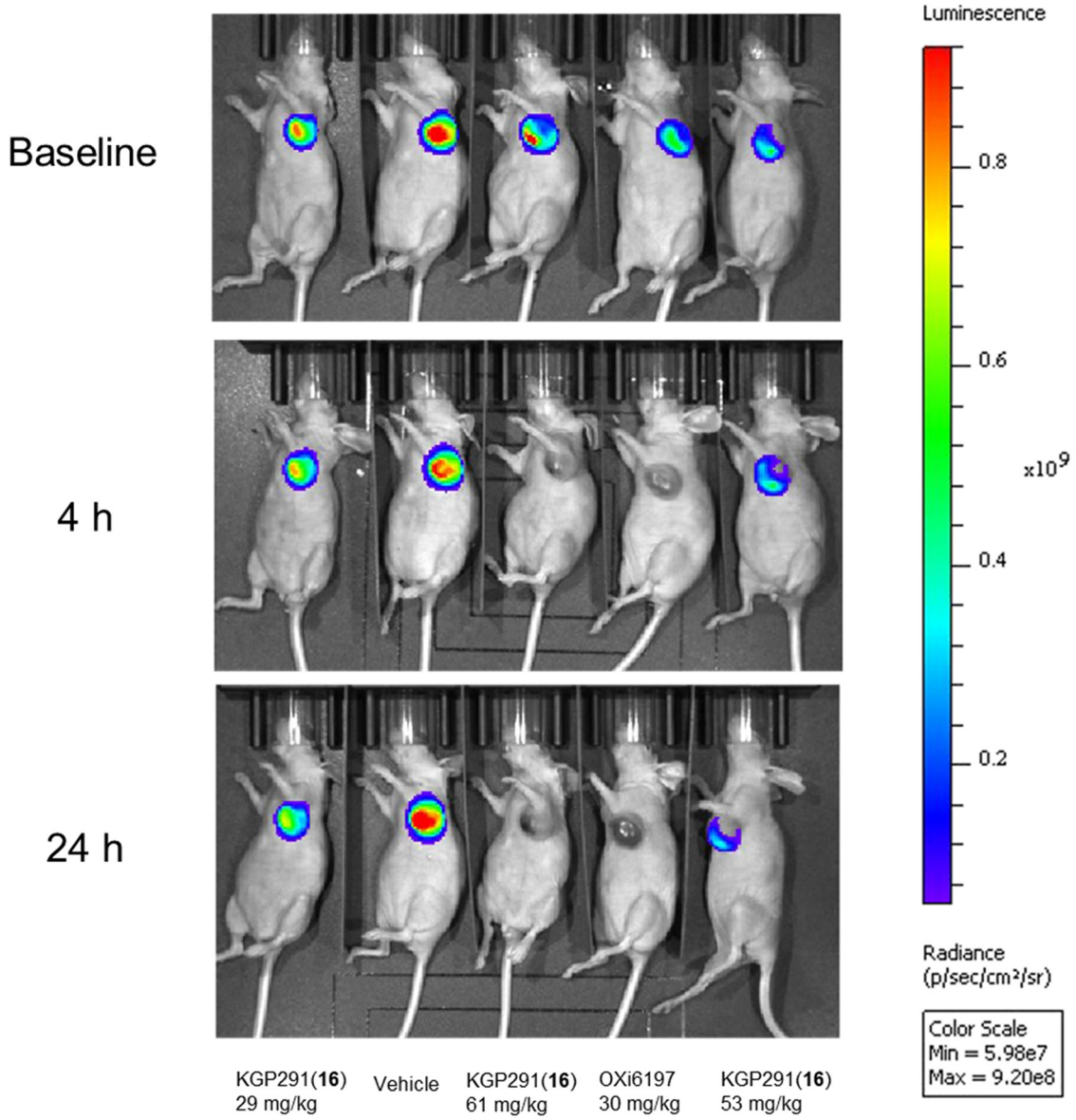

Fig. 5 BLI monitoring of tumor response to **KGP291**. Baseline shows mice at 20 min time point following administration of luciferin (120 mg kg^{-1}) subcutaneously to five athymic nude mice bearing orthotopic 4T1-luc tumors growing in frontal mammary fat pad. Immediately following baseline BLI, mice were treated by intraperitoneal injection as follows: (left to right) **KGP291** (29 mg kg^{-1}); vehicle (10% DMSO : 90% sesame oil); **KGP291** (61 mg kg^{-1}); **OXi6197** (30 mg kg^{-1}) in saline vehicle; **KGP291** (53 mg kg^{-1}). BLI was repeated at 4 h and 24 h after treatment.

of bioreductive triggers (nitrothiophene, nitroimidazole, and nitrophenyl) to generate corresponding BAPCs. Prodrug constructs were screened for inhibition of tubulin polymerization and percent inhibition of colchicine binding; all BAPCs demonstrated significant reduction in activity compared to the corresponding parent drug in these assays. BAPCs were evaluated for inhibition of growth (GI_{50}) of A549 human cancer cells under normoxic and hypoxic conditions (COY chamber) using an SRB assay. Selectivity for drug release under hypoxic conditions was determined by hypoxic cytotoxicity ratio (HCR), and compounds **13**, **15**, **16**, **20**, and **21** produced positive HCR values (10.9, 6.2, 7.8, 6.0, and 7.8 respectively). The indole BAPC series (**23**, **24** and **25**) showed exemplary HCR values (76.6, 34.9, and 82.2). Preliminary *in vivo* BLI evaluation of compound **16** (61 mg kg^{-1}) against orthotopic 4T1-luc tumors (nude mouse model) showed a dramatic decrease in signal after 4 h and continued signal reduction after 24 h. Evidence of vascular shutdown (imaged by BLI), suggests compound **16** and related BAPCs are promising candidates for further development as antiproliferative agents and VDAs.

4. Experimental section

4.1. Chemistry

4.1.1. General materials and methods. Dichloromethane (CH_2Cl_2), acetonitrile, dimethylformamide (DMF), methanol, ethanol (EtOH), and tetrahydrofuran (THF) were used in their anhydrous forms, as obtained from the chemical suppliers.

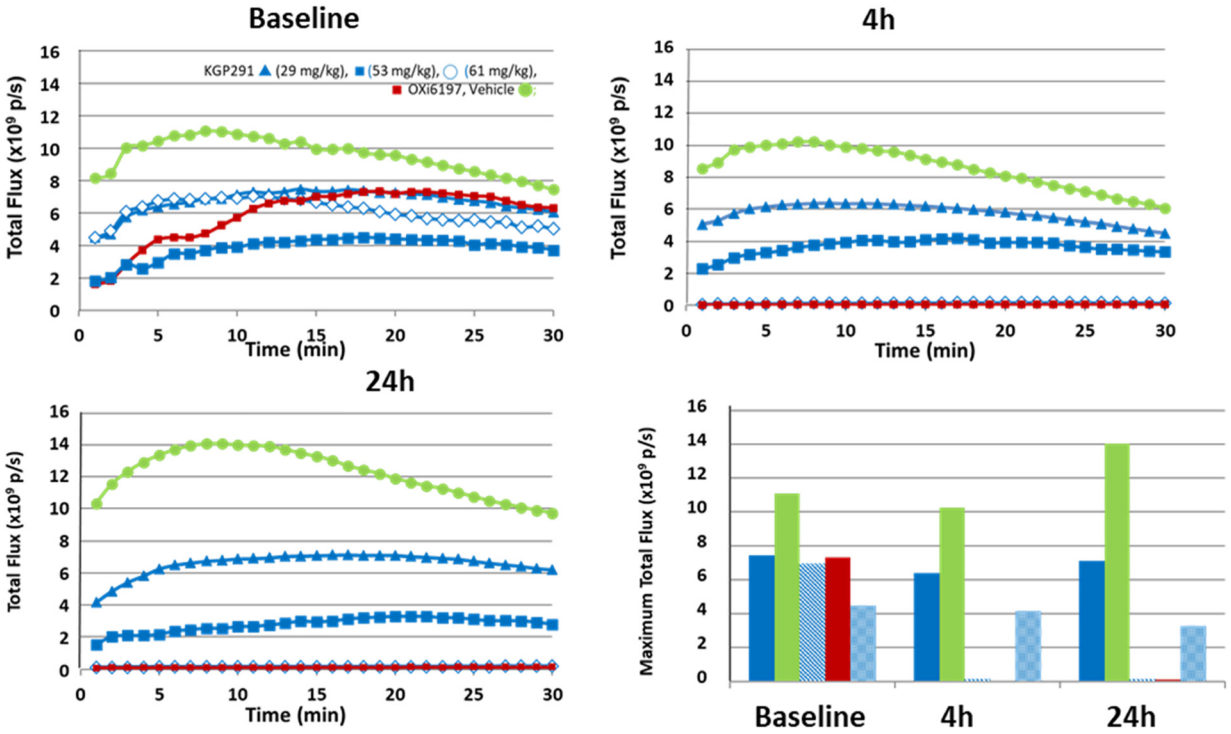

Fig. 6 Dynamic light emission time courses with respect to vascular disruption. Variation of signal intensity is shown at baseline, 4 h and 24 h. Mouse represented by lines with red squares received **OXi6197**; mouse represented by green circles received vehicle; mouse represented by solid blue triangles were treated with **KGP291** (29 mg kg^{-1}); mouse represented by solid blue squares received **KGP291** (53 mg kg^{-1}); and mouse represented by open blue diamonds received **KGP291** (61 mg kg^{-1}). At baseline, all tumors showed similar light emission kinetics (upper left). 4 h and 24 h later (upper right and lower left, respectively), the tumors receiving **OXi6197** and the highest dose of **KGP291** showed substantially reduced signal, while the tumors receiving vehicle alone and two lower doses of **KGP291** showed little change. The histogram (lower right) shows the maximum light emission for each dynamic curve. Following 61 mg kg^{-1} **KGP291**, BLI intensity was significantly reduced compared with lower doses or vehicle ($p < 0.05$).

Reactions were performed under an inert atmosphere using nitrogen gas, unless specified. Thin-layer chromatography (TLC) plates (precoated glass plates with silica gel 60 F254, 0.25 mm thickness) were used to monitor reactions. Purification of intermediates and products was carried out with a Biotage Isolera flash purification system using silica gel (200–400 mesh, 60 Å). Intermediates and products synthesized were characterized on the basis of their ^{1}H NMR (600 or 500 MHz) and ^{13}C NMR (151 or 126 MHz) spectroscopic data using a Bruker Avance III 600 MHz or a Varian VNMRs 500 MHz instrument. Spectra were recorded in $CDCl_3$, $(CD_3)_2SO$, or $(CD_3)_2CO$. All chemical shifts are expressed in ppm (δ), coupling constants (J) are presented in Hz, and peak patterns are reported as broad (br), singlet (s), doublet (d), triplet (t), quartet (q), septet (sept), double doublet (dd), and multiplet (m). Purity of the final compounds was further analyzed at 25 °C using an Agilent 1200 HPLC system with a diode-array detector (λ = 190–400 nm), a Zorbax XDB-C18 HPLC column (4.6–150 mm, 5 μm), and a Zorbax reliance cartridge guard-column; solvent A, acetonitrile, solvent B, H_2O; gradient, 50% A/50% B to 100% A/0% B over 0 to 30 min; post-time 10 min; flow rate 1.0 mL min^{-1}; injection volume 20 μL; monitored at wavelengths of 210, 254, 280, 300, and 320 nm. Mass spectrometry was carried out under positive ESI (electrospray ionization) using a Thermo Scientific LTQ Orbitrap Discovery instrument.

Experimental procedures for OXi6196, KGP18, OXi8006 and bioreductive triggers. Procedures for the synthesis of **OXi6196** (**2**), **KGP18** (**3**), **OXi8006** (**4**) and bioreductive triggers (**5–11**) can be found in our previously published work.[35–39,48,58]

Experimental procedures for the synthesis of BAPCs

*4.1.1.1. 2-(((2-Methoxy-5-(3,4,5-trimethoxyphenyl)-7,8-dihydronaphthalen-1-yl)oxy)methyl)-5-nitrothiophene (**12**).* **OXi6196** (**2**) (0.340 g, 1.00 mmol), (5-nitrothiophen-2-yl)methanol **5** (0.080 g, 0.500 mmol), and PPh_3 (0.267 g, 1.00 mmol) were dissolved in THF (2.0 mL) at room temperature. DEAD (0.158 mL, 1.00 mmol) was added dropwise, and the reaction mixture was stirred at 55 °C for 3.5 h. The reaction was cooled to room temperature, and the solvent was removed under reduced pressure. Purification by flash chromatography using a pre-packed (25 g) silica column [solvent A: EtOAc; solvent B: hexanes; gradient 0% A/100% B (1 CV), 0% A/100% B → 30% A/70% B (13 CV), 30% A/70% B (2 CV); flow rate: 75 mL min^{-1}; monitored at 254 and 280 nm] afforded compound **12** (0.040 g, 0.083 mmol, 17% yield) as a yellow oil. ^{1}H NMR ($(CD_3)_2CO$, 500 MHz): δ 7.98 (1H, d, J = 4.2 Hz), 7.24 (1H, dt, J = 4.2, 0.9 Hz), 6.87 (1H, d, J = 8.6 Hz), 6.84 (1H, d, J = 8.6 Hz), 6.58 (2H, s), 5.99 (1H, t, J = 4.7 Hz), 5.31 (2H, br s), 3.91 (3H, s), 3.81 (6H, s), 3.76

(3H, s), 2.85 (2H, t, J = 8.1 Hz), 2.29 (2H, td, J = 8.0, 4.7 Hz). ^{13}C NMR ($(CD_3)_2CO$, 151 MHz): δ 153.3, 151.8, 151.4, 149.8, 143.6, 139.5, 137.7, 136.3, 130.5, 128.8, 128.6, 125.9, 124.9, 122.1, 109.3, 106.1, 68.6, 59.7, 55.5, 55.2, 22.6, 21.1. HRMS: obsd 506.1244 [M + Na^+], calcd for $C_{25}H_{25}NNaO_7S^+$: 506.1244. HPLC purity 100%, retention time – 16.4 min.

*4.1.1.2. 2-(1-((2-Methoxy-5-(3,4,5-trimethoxyphenyl)-7,8-dihydronaphthalen-1-yl)oxy)ethyl)-5-nitrothiophene (**13**).* The procedure was similar to compound **12**, except that bioreductive trigger **6** was used instead of **5** to afford compound **13** (0.115 g, 0.231 mmol, 46% yield) as a yellow solid. ^{1}H NMR ($(CD_3)_2CO$, 500 MHz): δ 7.95 (1H, d, J = 4.2 Hz), 7.16 (1H, dd, J = 4.2, 0.9 Hz), 6.85 (1H, d, J = 8.6 Hz), 6.81 (1H, d, J = 8.6 Hz), 6.58 (2H, s), 5.98 (1H, t, J = 4.7 Hz), 5.68 (1H, qd, J = 6.4, 0.9 Hz), 3.87 (3H, s), 3.81 (6H, s), 3.75 (3H, s), 2.78 (2H, ddd, J = 10.8, 8.9, 6.7 Hz), 2.34–2.14 (2H, m), 1.71 (3H, d, J = 6.5 Hz). ^{13}C NMR ($(CD_3)_2CO$, 126 MHz): δ 155.6, 153.3, 151.9, 150.7, 142.2, 139.6, 136.4, 130.9, 128.7, 128.6, 125.0, 124.2, 121.9, 109.3, 106.1, 106.1, 74.8, 59.7, 55.5, 55.1, 27.7, 21.7, 21.3. HRMS: obsd 520.1400 [M + Na^+], calcd for $C_{26}H_{27}NNaO_7S^+$: 520.1400. HPLC purity 98.6%, retention time – 18.7 min. This compound was synthesized as a racemic mixture.

*4.1.1.3. 2-(2-((2-Methoxy-5-(3,4,5-trimethoxyphenyl)-7,8-dihydronaphthalen-1-yl)oxy)propan-2-yl)-5-nitrothiophene (**14**).* The procedure was similar to compound **12**, except that bioreductive trigger **7** was used instead of **5** to afford compound **14** (0.035 g, 0.068 mmol, 16%) as an orange solid. ^{1}H NMR ($(CD_3)_2CO$, 600 MHz): δ 7.87 (1H, d, J = 4.3 Hz), 7.03 (1H, d, J = 4.3 Hz), 6.70 (1H, d, J = 8.4 Hz), 6.58 (2H, s), 6.54 (1H, d, J = 8.4 Hz), 5.95 (1H, t, J = 4.7 Hz), 3.82 (3H, s), 3.80 (6H, s), 3.75 (3H, s), 2.81 (2H, t, J = 7.9 Hz), 2.30 (2H, td, J = 7.9, 4.7 Hz), 1.63 (6H, s). ^{13}C NMR ($(CD_3)_2CO$, 126 MHz): δ 166.2, 153.1, 146.6, 142.5, 139.9, 137.5, 136.8, 129.3, 128.6, 124.5, 122.4, 121.4, 117.1, 107.8, 106.1, 70.9, 59.7, 55.5, 55.3, 31.4, 31.3, 22.7, 20.2. HPLC purity 91.2%, retention time – 21.6 min. While purification beyond 91.2% by flash chromatography proved challenging, there was no parent agent (to the best of our knowledge) as part of the impurities, thus this did not influence the biological evaluation.

*4.1.1.4. 5-(((2-Methoxy-5-(3,4,5-trimethoxyphenyl)-7,8-dihydronaphthalen-1-yl)oxy)methyl)-1-methyl-2-nitro-1H-imidazole (**15**).* **OXi6196** (**2**) (0.363 g, 1.06 mmol), (1-methyl-2-nitro-1*H*-imidazol-5-yl)methanol **8** (0.200 g, 1.27 mmol), and DIAD (0.280 mL, 1.43 mmol) were dissolved in THF (70 mL) at room temperature. PPh_3 (0.557 g, 2.12 mmol) was added, and the reaction mixture was stirred for 48 h. The solvent was removed under reduced pressure. Purification by flash chromatography using a pre-packed (50 g) silica column [solvent A: EtOAc; solvent B: hexanes; gradient 10% A/90% B (1 CV), 10% A/90% B → 80% A/20% B (13 CV), 80% A/20% B (2 CV); flow rate: 50 mL min^{-1}; monitored at 254 and 280 nm] afforded compound **15** (0.179 g, 0.371 mmol, 35% yield) as a yellow solid. ^{1}H NMR ($CDCl_3$, 600 MHz): δ 7.14 (1H, s), 6.85 (1H, d, J = 8.5 Hz), 6.69 (1H, d, J = 8.5 Hz), 6.54 (2H, s), 5.97 (1H, t, J = 4.6 Hz), 5.01 (2H, s), 4.24 (3H, s), 3.89 (3H, s), 3.85 (3H, s), 3.85 (6H, s), 2.76 (2H, t, J = 7.9 Hz), 2.31 (2H, td, J = 7.8, 4.6 Hz). ^{13}C NMR ($CDCl_3$, 151 MHz): δ 153.0, 151.6, 143.0, 139.4, 137.2, 136.4, 133.9, 130.7, 129.1, 129.0, 125.4, 122.6, 109.0, 107.2, 105.8, 63.0, 61.0, 56.2, 55.6, 34.6, 22.8, 21.1. HRMS: obsd 504.1740 [M + Na^+], calcd for $C_{25}H_{27}N_3NaO_7^+$: 504.1741. HPLC purity 96.2%, retention time – 7.3 min.

*4.1.1.5. 5-(1-((2-Methoxy-5-(3,4,5-trimethoxyphenyl)-7,8-dihydronaphthalen-1-yl)oxy)ethyl)-1-methyl-2-nitro-1H-imidazole (**16**).* The procedure was similar to compound **15**, except that bioreductive trigger **9** was used instead of **8** to afford compound **16** (0.0694 g, 0.140 mmol, 24%) as a yellow solid. ^{1}H NMR ($CDCl_3$, 600 MHz): δ 7.14 (1H, s), 6.77 (1H, d, J = 8.5 Hz), 6.62 (1H, d, J = 8.6 Hz), 6.47 (2H, s), 5.91 (1H, t, J = 4.6 Hz), 5.53 (1H, q, J = 6.6 Hz), 4.11 (3H, s), 3.82 (3H, s), 3.79 (3H, s), 3.78 (6H, s), 2.69 (2H, td, J = 9.3, 6.8 Hz), 2.27–2.14 (2H, m), 1.61 (3H, d, J = 6.6 Hz). ^{13}C NMR ($(CD_3)_2CO$, 126 MHz): δ 153.3, 152.0, 141.6, 139.6, 138.8, 137.6, 136.3, 131.6, 128.7, 126.3, 125.0, 122.0, 109.2, 106.0, 68.9, 59.7, 55.5, 55.1, 34.1, 22.6, 21.7, 17.6. HRMS: obsd 496.2077 [M + H^+], calcd for $C_{26}H_{30}N_3O_7^+$: 496.2078. HPLC purity 94.9%, retention time – 10.0 min. This compound was synthesized as a racemic mixture.

*4.1.1.6. 2-[2-Methoxy-5-(3′,4′,5′-trimethoxyphenyl)-7,8-dihydronaphthalen-1-yl-oxymethyl]-1-methyl-5-nitro-1H-imidazole (**17**).* The procedure was similar to compound **12**, except that bioreductive trigger **10** was used instead of **5** to afford compound **17** (0.090 g, 0.187 mmol, 37%); ^{1}H NMR ($CDCl_3$, 500 MHz): δ 7.98 (1H, s), 6.85 (1H, d, J = 8.6 Hz), 6.69 (1H, d, J = 8.6 Hz), 6.54 (2H, br s, Ar*H*), 5.98 (1H, t, J = 4.7 Hz), 5.10 (2H, s), 4.24 (3H, s), 3.89 (3H, s), 3.85 (9H, s), 2.80 (2H, t, J = 7.8 Hz), 2.33 (2H, m); ^{13}C NMR ($CDCl_3$, 125 MHz) δ 153.0, 151.6, 148.4, 143.1, 139.4, 137.2, 136.4, 131.8, 130.9, 129.2, 125.5, 122.7, 108.9, 105.8, 66.2, 60.9, 56.1, 55.6, 33.9, 22.8, 21.0; HRMS (EI): obsd 481.1851 [M^+], calcd for $C_{25}H_{27}N_3O_7^+$: 481.1849. HPLC purity 93.0%, retention time – 16.5 min. While purification beyond 93.0% by flash chromatography proved challenging, there was no parent agent (to the best of our knowledge) as part of the impurities, thus this did not influence the biological evaluation.

*4.1.1.7. 7-Methoxy-8-(4-nitrobenzyloxy)-4-(3′,4′,5′-trimethoxyphenyl)-1,2-dihydronaphthalene (**18**).* The procedure was similar to compound **12**, except that bioreductive trigger **11** was used instead of **5** to afford compound **18** (0.100 g, 0.210 mmol, 42%); ^{1}H NMR ($CDCl_3$, 500 MHz): δ 8.26 (2H, d, J = 8.8 Hz), 7.68 (2H, d, J = 8.6 Hz), 6.84 (1H, d, J = 8.6 Hz), 6.71 (1H, d, J = 8.6 Hz), 6.55 (2H, br s), 5.97 (1H, t, J = 4.7 Hz), 5.11 (2H, s), 3.89 (3H, s), 3.87 (3H, s), 3.85 (6H, s), 2.85 (2H, t, J = 8.0 Hz), 2.31 (2H, m); ^{13}C NMR ($CDCl_3$, 125 MHz) δ 153.0, 151.9, 147.6, 145.4, 144.0, 139.5, 137.2, 136.6, 130.7, 129.0, 128.2, 125.4, 123.6, 122.1, 109.1, 105.9, 73.2, 61.0, 56.2, 55.7, 22.9, 21.3; HRMS (EI): obsd 477.1794 [M^+], calcd for $C_{27}H_{27}NO_7^+$: 477.1788. HPLC purity 100%, retention time – 16.50 min.

*4.1.1.8. 2-(((3-Methoxy-9-(3,4,5-trimethoxyphenyl)-6,7-dihydro-5H-benzo[7]annulen-4-yl)oxy)methyl)-5-nitrothiophene (**19**).* **KGP18** (**3**) (0.301 g, 0.844 mmol), (5-nitrothiophen-2-yl)methanol **5**

(0.129 g, 0.810 mmol), and PPh_3 (0.435 g, 1.66 mmol) were dissolved in CH_2Cl_2 (7 mL). ADDP (0.333 g, 1.32 mmol) was added, and the solution was stirred at room temperature for 12 h. The solvent was removed under reduced pressure. Purification on silica gel using isocratic 7.5% EtOAc: 92.5% hexanes as eluent, followed by recrystallization using Et_2O, afforded compound **19** (0.050 g, 0.010 mmol, 12% yield) as a yellow solid. ^{1}H NMR ($CDCl_3$, 500 MHz): δ 7.85 (1H, d, J = 4.2 Hz), 7.03 (1H, d, J = 4.2 Hz), 6.83 (1H, d, J = 8.6 Hz), 6.80 (1H, d, J = 8.6 Hz), 6.48 (2H, s), 6.34 (1H, t, J = 7.3 Hz), 5.22 (2H, d, J = 0.5 Hz), 3.92 (3H, s), 3.86 (3H, s), 3.81 (6H, s), 2.73 (2H, t, J = 6.8 Hz), 2.07 (2H, p, J = 7.0 Hz), 1.93 (2H, q, J = 7.0 Hz). ^{13}C NMR ($CDCl_3$, 126 MHz): δ 152.9, 151.8, 151.1, 149.2, 143.8, 142.6, 138.2, 137.5, 135.9, 134.0, 128.2, 127.3, 126.1, 125.0, 109.4, 105.3, 69.4, 60.9, 56.2, 55.7, 34.4, 25.5, 24.4. HRMS: obsd 520.1394 [M + Na^+], calcd for $C_{26}H_{27}NNaO_7S^+$: 520.1400. HPLC purity 98.8%, retention time – 16.5 min.

4.1.1.9. 2-(1-((3-Methoxy-9-(3,4,5-trimethoxyphenyl)-6,7-dihydro-5H-benzo[7]annulen-4-yl)oxy)ethyl)-5-nitrothiophene (20). **KGP18** (**3**) (1.50 g, 4.20 mmol), 1-(5-nitrothiophen-2-yl)ethan-1-ol **6** (0.650 g, 3.75 mmol), and PPh_3 (1.37 g, 7.29 mmol) were dissolved in CH_2Cl_2 (40 mL). DIAD (1.15 mL, 5.08 mmol) was added, and the solution was stirred at room temperature for 12 h. The solvent was removed under reduced pressure, and the crude mixture was purified on silica gel using isocratic 5% EtOAc : 95% hexanes as eluent, followed by recrystallization using Et_2O to afford compound **20** (0.869 g, 1.70 mmol, 45% yield) as a yellow solid. ^{1}H NMR ($CDCl_3$, 500 MHz): δ 7.81 (1H, d, J = 4.4 Hz), 6.94 (1H, dd, J = 4.2, 0.7 Hz), 6.80 (1H, d, J = 8.6 Hz), 6.77 (1H, d, J = 8.6 Hz), 6.45 (2H, s), 6.32 (1H, t, J = 7.1 Hz), 5.62 (1H, qd, J = 6.4, 0.7 Hz), 3.87 (3H, s), 3.86 (3H, s), 3.80 (6H, s), 2.74 (1H, m), 2.64 (1H, m), 2.06 (1H, m), 1.91 (3H, m), 1.73 (3H, d, J = 6.6 Hz). ^{13}C NMR ($CDCl_3$, 126 MHz): δ 155.3, 152.9, 151.1, 142.6, 142.4, 138.3, 137.4, 136.6, 134.0, 128.1, 127.3, 125.8, 123.3, 109.4, 105.2, 74.6, 60.9, 56.1, 55.6, 34.1, 25.6, 24.4, 21.8. HRMS: obsd 534.1556 [M + H^+], calcd for $C_{27}H_{29}NNaO_7S^+$: 534.1557. HPLC purity 99.0%, retention time – 20.1 min. This compound was synthesized as a racemic mixture.

4.1.1.10. 5-(((3-Methoxy-9-(3,4,5-trimethoxyphenyl)-6,7-dihydro-5H-benzo[7]annulen-4-yl)oxy)methyl)-1-methyl-2-nitro-1H-imidazole (21). **KGP18** (**3**) (0.250 g, 0.702 mmol), (1-methyl-2-nitro-1*H*-imidazol-5-yl)methanol **8** (0.123 g, 0.842 mmol), and DEAD (0.144 mL, 0.913 mmol) were dissolved in CH_2Cl_2 (60 mL). PPh_3 (0.368 g, 1.40 mmol) was added to the solution, and the reaction mixture was stirred at room temperature for 48 h. The solvent was removed under reduced pressure. Purification by flash chromatography using a pre-packed (50 g) silica column [solvent A: EtOAc; solvent B: hexanes; gradient 10% A/90% B (1 CV), 10% A/90% B → 80% A/20% B (13 CV), 80% A/20% B (2 CV); flow rate: 50 mL min^{-1}; monitored at 254 and 280 nm] afforded compound **21** (0.143 g, 0.288 mmol, 41% yield) as an orange crystal. ^{1}H NMR ($CDCl_3$, 600 MHz): δ 7.15 (1H, s), 6.84 (1H, d, J = 8.5 Hz), 6.79 (1H, d, J = 8.5 Hz), 6.46 (2H, s), 6.34 (1H, t, J = 7.3 Hz), 5.05 (2H, s), 4.25 (3H, s), 3.89 (3H, s), 3.86 (3H, s), 3.80 (6H, s), 2.68 (2H, t, J = 6.9 Hz), 2.07–1.99 (2H, m), 1.93 (2H, q, J = 7.1 Hz). ^{13}C NMR (CDCl3, 151 MHz): δ 152.9, 151.2, 143.4, 142.6, 138.1, 137.6, 135.9, 134.2, 134.0, 128.8, 127.3, 126.4, 109.3, 105.3, 63.6, 60.9, 56.2, 55.6, 34.6, 34.4, 25.5, 24.4. HRMS: obsd 518.1898 [M + Na^+], calcd for $C_{26}H_{29}N_3NaO_7^+$: 518.1898. HPLC purity 98.1%, retention time – 10.7 min.

4.1.1.11. 5-(1-((3-Methoxy-9-(3,4,5-trimethoxyphenyl)-6,7-dihydro-5H-benzo[7]annulen-4-yl)oxy)ethyl)-1-methyl-2-nitro-1H-imidazole (22). The procedure was similar to compound **20**, except that bioreductive trigger **9** was used instead of **6** to afford compound **22** (0.122 g, 0.239 mmol, 34% yield) as an orange solid. ^{1}H NMR ($CDCl_3$, 600 MHz): δ 7.14 (1H, s), 6.75 (1H, d, J = 8.5 Hz), 6.71 (1H, d, J = 8.5 Hz), 6.38 (2H, s), 6.26 (1H, t, J = 7.0 Hz), 5.57 (1H, q, J = 6.6 Hz), 4.09 (3H, s), 3.81 (3H, s), 3.79 (3H, s), 3.73 (6H, s), 2.63 (1H, dt, J = 12.6, 6.3 Hz), 2.54 (1H, dt, J = 13.7, 6.8 Hz), 2.05–1.97 (1H, m), 1.85 (3H, m), 1.64 (3H, d, J = 6.6 Hz). ^{13}C NMR ($CDCl_3$, 151 MHz): δ 152.9, 151.1, 146.3, 142.5, 141.7, 138.6, 138.2, 137.5, 136.8, 134.3, 127.4, 126.7, 126.1, 109.2, 105.3, 68.7, 60.9, 56.2, 55.5, 34.7, 34.1, 25.6, 24.3, 18.4. HRMS: obsd 532.2054 [M + Na^+], calcd for $C_{27}H_{31}N_3NaO_7^+$: 532.2053. HPLC purity 97.5%, retention time – 11.5 min. This compound was synthesized as a racemic mixture.

4.1.1.12. (6-Methoxy-2-(4-methoxy-3-((5-nitrothiophen-2-yl)methoxy)phenyl)-1H-indol-3-yl)(3,4,5-trimethoxyphenyl)methanone (23). The procedure was similar to compound **20**, except that **OXi8006** (**4**) was used instead of **KGP18** (**3**) and bioreductive trigger **5** was used instead of **6** to afford compound **23** (0.080 g, 0.11 mmol, 13% yield) as a yellow solid. ^{1}H NMR ($CDCl_3$, 500 MHz): δ 8.62 (1H, s), 7.81 (1H, d, J = 9.5 Hz), 7.78 (1H, d, J = 4.0 Hz), 7.10 (1H, dd, J = 8.0, 2.0 Hz), 6.99 (2H, s), 6.95 (1H, d, J = 4.0 Hz), 6.89 (2H, m), 6.85 (1H, d, J = 2.0 Hz), 6.81 (1H, d, J = 8.0 Hz), 4.91 (2H, s), 3.85 (3H, s), 3.83 (3H, s), 3.82 (3H, s), 3.67 (6H, s). ^{13}C NMR ($CDCl_3$, 126 MHz): δ 192.0, 157.5, 152.8, 151.8, 150.6, 148.1, 147.0, 141.8, 141.6, 136.5, 134.9, 128.5, 125.1, 124.9, 123.1, 122.9, 122.5, 117.3, 113.0, 111.94, 111.87, 107.5, 94.7, 66.9, 61.1, 56.2, 56.1, 55.8. HRMS: obsd 605.1587 [M + H^+], calcd for $C_{31}H_{29}N_2O_9S^+$: 605.1588. HPLC purity 94.7%, retention time – 7.74 min.

4.1.1.13. (6-Methoxy-2-(4-methoxy-3-(1-(5-nitrothiophen-2-yl)ethoxy)phenyl)-1H-indol-3-yl)(3,4,5-trimethoxyphenyl)methanone (24). The procedure was similar to compound **20**, except that **OXi8006** (**4**) was used instead of **KGP18** (**3**) to afford compound **24** (0.19 g, 0.31 mmol, 32% yield) as a yellow solid. ^{1}H NMR ($CDCl_3$, 500 MHz): δ 8.97 (1H, s), 7.75 (1H, d, J = 9.5 Hz), 7.68 (1H, d, J = 4.0 Hz), 7.05 (1H, dd, J = 8.0, 2.0 Hz), 6.99 (2H, s), 6.86 (1H, d, J = 2.0 Hz), 6.84 (2H, m), 6.79 (1H, dd, J = 4.0, 1.0 Hz), 6.71 (1H, d, J = 8.0 Hz), 5.13 (1H, q, J = 6.0 Hz), 3.82 (3H, s), 3.80 (3H, s), 3.78 (3H, s), 3.66 (6H, s), 1.53 (3H, d, J = 6.0 Hz). ^{13}C NMR ($CDCl_3$, 126 MHz): δ 191.9, 157.4, 155.3, 152.7, 151.4, 150.9, 146.1, 141.7, 141.5, 136.5, 134.7, 128.6, 124.8, 123.4, 123.1, 123.1, 122.4, 119.7, 112.9, 112.1, 111.8, 107.4, 94.6, 74.5, 61.0, 56.2, 56.0, 55.7, 22.9. HRMS: obsd 619.1742 [M + H^+], calcd for $C_{32}H_{31}N_2O_9S^+$: 619.1745. HPLC purity 85.8%, retention time – 15.73 min. While purification beyond 85.8% by flash chromatography proved challenging, there was no parent agent (to the best of our knowledge) as part of the impurities, thus this did not

influence the biological evaluation. This compound was synthesized as a racemic mixture.

4.1.1.14. (6-Methoxy-2-(4-methoxy-3-((2-(5-nitrothiophen-2-yl) propan-2-yl)oxy)phenyl)-1H-indol-3-yl)(3,4,5-trimethoxyphenyl) methanone (25). **OXi8006** (**4**) (0.50 g, 1.08 mmol), 2-(5-nitrothiophen-2-yl)propan-2-ol **7** (0.22 g, 1.15 mmol) and ADDP (0.27 g, 1.08 mmol) were dissolved in benzene (10 mL). PBu_3 (0.27 mL, 1.08 mmol) was added dropwise to the solution and the reaction mixture was stirred at room temperature for 24 h. The solvent was removed under reduced pressure. Purification by flash chromatography using a pre-packed (50 g) silica gel column [solvent A, EtOAc, solvent B, hexanes; gradient 5% A/95% B (1 CV), 5% A/95% B → 40% A/60% B (12 CV), 40% A/60% B (1 CV); flow rate, 25 mL min^{-1}; monitored at 254 and 280 nm] afforded compound **25** (0.03 g, 0.05 mmol, 5% yield) as a yellow solid. ^1H NMR ($CDCl_3$, 500 MHz): δ 8.68 (1H, s), 7.67 (1H, d, J = 9.0 Hz), 7.65 (1H, d, J = 4.0 Hz), 7.16 (1H, dd, J = 8.5, 2.0 Hz), 7.03 (2H, s), 6.87 (1H, d, J = 2.0 Hz), 6.84 (2H, m), 6.78 (1H, d, J = 8.5 Hz), 6.76 (1H, d, J = 4.5 Hz), 3.85 (3H, s), 3.83 (3H, s), 3.74 (3H, s), 3.71 (6H, s), 1.51 (6H, s). ^{13}C NMR ($CDCl_3$, 126 MHz): δ 191.5, 161.1, 157.4, 154.1, 152.8, 150.7, 143.4, 141.6, 141.3, 136.4, 134.5, 128.4, 125.4, 124.8, 124.8, 123.1, 122.4, 122.2, 112.9, 112.2, 111.8, 107.6, 94.6, 80.7, 61.0, 55.3, 55.8, 55.8, 28.7. HRMS: obsd 633.1899 [M + H^+], calcd for $C_{33}H_{33}N_2O_9S^+$: 633.1901. HPLC purity 74.5%, retention time – 16.37 min. While purification beyond 74.5% by flash chromatography proved challenging, there was no parent agent (to the best of our knowledge) as part of the impurities, thus this did not influence the biological evaluation.

4.2. Biological evaluation

4.2.1. Cell culture. A549 cells (human non-small-cell lung carcinoma, ATCC) were cultured in MEM-alpha medium containing 10% fetal bovine serum (FBS), 17 mM D-glucose, 1% glutamine, and 1% gentamycin sulfate. For the bioreductive assay, the same medium was used with the addition of 0.02 mM 2′-deoxycytidine hydrochloride. Cells were maintained in a log growth phase in a humidified 37 °C incubator under 95% air plus 5% CO_2.

4.2.2. Differential cytotoxicity. The bioreductive assay was modified from Jaffar *et al.*[55,77] For the anoxic assay, A549 cells were cultured in a Coy chamber in medium that had been preconditioned in the anaerobic chamber. Cells were plated at 6000 cells/100 μL per well into 96-well plates that had been degassed in the anaerobic chamber and allowed to attach for 2 h. Compounds to be tested were serially diluted in preconditioned medium from 10 mg mL^{-1} stock solutions in DMSO to 2× the final concentrations; 100 μL was added per well in duplicate for each experiment. The final concentrations of control and test compounds ranged from 50 μg mL^{-1} to 5 pg mL^{-1}. Plates were incubated for 4 h under anaerobic conditions and then either for 48 h under aerobic conditions without media change, or for 120 h under aerobic conditions after removal and replacement of media containing drug, prior to sulforhodamine B (SRB)[78–81] determination of cytotoxicity as previously reported.[22,23,55,78–83] Briefly, treated and control cells were fixed with 10% trichloroacetic acid, stained with 0.4% SRB dye for 30 min, and subsequently washed 4 times with 1% acetic acid in water. The plates were air dried, and the protein-bound SRB dye was solubilized with 10 mM Tris base. The plates were read at 540 nm and 630 nm (to adjust for background) with an automated Biotek Elx800 plate reader. IC_{50} values were determined with Excel software.[80] An identical procedure was used for the normoxic arm of the assay with the exception that all incubations were carried out under 95% air plus 5% CO_2. Tirapazamine was used as a positive control, as previously described.[22,23,82]

4.2.3. NADPH-cytochrome P450 oxidoreductase cleavage Assay.[55,84]. The enzymatic activity of rat NADPH-cytochrome P450 oxidoreductase supersome (Corning) was assessed with cytochrome c as substrate and protocatechuic acid (PCA, 3,4-dihydroxybenzoic acid). For the bioreductive enzyme assay,[54,55] BAPC prodrugs were diluted from 10 mM stock solutions in DMSO and added to 200 mM pH 7.4 potassium phosphate buffer containing 0.1% Triton X-100 (to facilitate BAPC solubility) and 400 μM freshly dissolved protocatechuic acid. The resulting solution was evacuated and flushed with nitrogen (3 times) followed by the addition of protocatechuate 3,4-dioxygenase (PCD, Sigma-Aldrich) to react with substrate PCA to remove remaining traces of O_2. POR and NADPH were then introduced sequentially. The anaerobic reaction mixture was incubated for designated times at 37 °C, cooled on ice, and treated with a 2× volume of acetonitrile to precipitate proteins. After centrifugation and syringe (0.2 μm) filtration, the samples were analyzed by HPLC using various gradients of acetonitrile/water for elution. Solutions without the POR enzyme were used as controls for stability studies. Standard curves were determined for each substrate and product for quantitation.

4.2.4. Colchicine binding assay. Inhibition of [^3H]colchicine binding to tubulin was measured using 100 μL reaction mixtures containing 1.0 μM tubulin, 5.0 μM [^3H]colchicine (from Perkin-Elmer), 5% (v/v) dimethyl sulfoxide, potential inhibitors at 1.0 or 5.0 μM, as indicated, and components that stabilize the colchicine binding activity of tubulin (1.0 M monosodium glutamate [adjusted to pH 6.6 with HCl in a 2.0 M stock solution], 0.5 mg mL^{-1} bovine serum albumin, 0.1 M glucose-1-phosphate, 1.0 mM $MgCl_2$, and 1.0 mM GTP). Incubation was for 10 min at 37 °C, when the binding reaction in control reaction mixtures is 40–60% complete. Reactions were stopped with 2.0 mL of ice-cold water, and the reaction mixtures were placed on ice. Each sample was poured onto a stack of two DEAE-cellulose filters (Whatman), followed by 6 mL of ice-cold water. The samples were aspirated under reduced vacuum. The filters were washed three times with 2 mL water and placed into vials containing 5 mL of Biosafe II scintillation cocktail. Samples were counted 18 h later in a Beckman scintillation counter. Samples with inhibitors were compared to samples with no inhibitor, and percent inhibition was determined. All samples were corrected for radiolabel bound to the filters in the absence of tubulin.

4.2.5. Inhibition of tubulin polymerization. Tubulin polymerization experiments were performed in 0.25 mL reaction mixtures (final volume) that contained 1 mg mL^{-1} (10 μM) purified bovine brain tubulin, 0.8 M monosodium glutamate (pH 6.6), 4% (v/v) dimethyl sulfoxide, 0.4 mM GTP, and different compound concentrations. All reaction components except GTP were preincubated for 15 min at 30 °C in 0.24 mL. The mixtures were cooled to 0 °C, and 10 μL of 10 mM GTP was added. Reaction mixtures were transferred to cuvettes held at 0 °C in Beckman DU-7400 or DU-7500 spectrophotometers equipped with electronic temperature controllers. The temperature was jumped to 30 °C, taking about 30 s, and polymerization was followed at 350 nm for 20 min. The IC_{50} was defined as the compound concentration that inhibited extent of polymerization by 50% after 20 min.

4.2.6. *In vivo* bioluminescence imaging (BLI) with KGP291 (16). 4T1-luc cells [1×10^6 in 100 μL PBS with 50% Matrigel® (original cell line from ATCC, with transfected cell line provided by Dr. Edward Graves, Stanford University)] were injected directly into the left upper mammary fat pad of five female athymic nude mice. Tumors were allowed to grow over about 10 days, and then BLI was performed using an IVIS® Spectrum system (Perkin-Elmer (Xenogen), Alameda, CA), as described in detail previously.[55] Briefly, D-luciferin (128 mg kg^{-1} sodium salt in PBS in a total volume of 80 μL; Gold Biotechnology Inc., St. Louis, MO) was administered subcutaneously (SC) in the foreback neck region. Immediately after luciferin injection, a series of BLI images was acquired over a period of 30 min using auto exposure time. Following baseline BLI, mice were injected intraperitoneally (IP) respectively with either 29, 53, or 61 mg kg^{-1} of **KGP291** in vehicle (10% DMSO : 90% sesame oil). In addition, the vehicle and 30 mg kg^{-1} OXi6197 (also called **KGP04**)[45] in vehicle were used as controls. Dynamic BLI was repeated 4 and 24 h post-treatment with administration of fresh luciferin on each occasion. All animal experiments and procedures were carried out in accordance with the State of Texas and United States (US) Federal guidelines and were approved by the Institutional Animal Care and Use Committee (IACUC) of the University of Texas Southwestern Medical Center under APN101222 and APN102169.

Conflicts of interest

A portion of the research presented in this manuscript was funded by Mateon Therapeutics, Inc. (formerly OXiGENE Inc.), and this previous relationship is properly indicated in the Acknowledgements section. In addition, one of the authors (KGP) was formerly a paid consultant with Mateon Therapeutics, Inc. and is a current shareholder. While Mateon Therapeutics (OXiGENE Inc.) no longer exists as a corporate entity, we appreciated the long-term scientific collaboration and note that there is no actual conflict of interest associated with the scientific content and data presented in this manuscript.

Data availability

Supplementary information: Details regarding the synthesis of additional analogues, further biological evaluation, and compound characterization are provided in the SI. See DOI: https://doi.org/10.1039/D5MD00564G.

Acknowledgements

Portions of this study are reported in Ph.D. dissertations by the co-authors.[85] The authors are grateful to the Cancer Prevention and Research Institute of Texas (CPRIT, Grant No. RP140399 to K. G. P., M. L. T., R. P. M.), the National Cancer Institute of the National Institutes of Health [Grant Numbers: R01CA140674 and R01CA244579 (to K. G. P., M. L. T., R. P. M.) and R01CA238624 (to K. G. P., M. L. T)], and Mateon Therapeutics, Inc. (grant to K. G. P., M. L. T.) for their financial support of this project. BLI was facilitated by the Southwestern Small Animal Imaging Resource supported in part by the NIH Comprehensive Cancer Center Grant P30 CA142543 and a Shared Instrumentation Grant 1S10 RR024757. The authors are grateful to Dr. David (Dai) Chaplin for his inspirational vision to investigate hypoxia-selective prodrugs, and Dr. Tracy E. Strecker (Baylor University) for his technical support. We would like to honor Nathaneal Lutz posthumously for his contribution to this work. The authors also thank Dr. Michelle Nemec (Director) for the use of the shared Molecular Biosciences Center at Baylor University and Dr. Alejandro Ramirez (Mass Spectrometry Core Facility, Baylor University). This research was supported in part by the Developmental Therapeutics Program in the Division of Cancer Treatment and Diagnosis of the National Cancer Institute, which includes federal funds under Contract No. HHSN261200800001E. The content of this publication does not necessarily reflect the views or policies of the Department of Health and Human Services, nor does mention of trade names, commercial products, or organizations imply endorsement by the U.S. Government.

References

1 D. Hanahan and R. A. Weinberg, Hallmarks of cancer: the next generation, *Cell*, 2011, **144**, 646–674.
2 D. W. Siemann, The unique characteristics of tumor vasculature and preclinical evidence for its selective disruption by Tumor-Vascular Disrupting Agents, *Cancer Treat. Rev.*, 2011, **37**, 63–74.
3 L. H. Gray, A. D. Conger, M. Ebert, S. Hornsey and O. C. Scott, The concentration of oxygen dissolved in tissues at the time of irradiation as a factor in radiotherapy, *Br. J. Radiol.*, 1953, **26**, 638–648.
4 J. L. Tatum, G. J. Kelloff, R. J. Gillies, J. M. Arbeit, J. M. Brown, K. S. Chao, J. D. Chapman, W. C. Eckelman, A. W. Fyles, A. J. Giaccia, R. P. Hill, C. J. Koch, M. C. Krishna, K. A. Krohn, J. S. Lewis, R. P. Mason, G. Melillo, A. R. Padhani, G. Powis, J. G. Rajendran, R. Reba, S. P. Robinson, G. L. Semenza, H. M. Swartz, P. Vaupel, D. Yang, B. Croft, J. Hoffman, G. Liu, H. Stone and D. Sullivan, Hypoxia:

importance in tumor biology, noninvasive measurement by imaging, and value of its measurement in the management of cancer therapy, *Int. J. Radiat. Biol.*, 2006, **82**, 699–757.

5 W. R. Wilson and M. P. Hay, Targeting hypoxia in cancer therapy, *Nat. Rev. Cancer*, 2011, **11**, 393–410.

6 F. W. Hunter, B. G. Wouters and W. R. Wilson, Hypoxia-activated prodrugs: paths forward in the era of personalised medicine, *Br. J. Cancer*, 2016, **114**, 1071–1077.

7 D. C. Singleton, A. Macann and W. R. Wilson, Therapeutic targeting of the hypoxic tumour microenvironment, *Nat. Rev. Clin. Oncol.*, 2021, **18**, 751–772.

8 J. X. Duan, H. Jiao, J. Kaizerman, T. Stanton, J. W. Evans, L. Lan, G. Lorente, M. Banica, D. Jung, J. Wang, H. Ma, X. Li, Z. Yang, R. M. Hoffman, W. S. Ammons, C. P. Hart and M. Matteucci, Potent and highly selective hypoxia-activated achiral phosphoramidate mustards as anticancer drugs, *J. Med. Chem.*, 2008, **51**, 2412–2420.

9 M. Tercel, A. E. Lee, A. Hogg, R. F. Anderson, H. H. Lee, B. G. Siim, W. A. Denny and W. R. Wilson, Hypoxia-selective antitumor agents. 16. Nitroarylmethyl quaternary salts as bioreductive prodrugs of the alkylating agent mechlorethamine, *J. Med. Chem.*, 2001, **44**, 3511–3522.

10 J. D. Sun, Q. Liu, J. Wang, D. Ahluwalia, D. Ferraro, Y. Wang, J. X. Duan, W. S. Ammons, J. G. Curd, M. D. Matteucci and C. P. Hart, Selective tumor hypoxia targeting by hypoxia-activated prodrug TH-302 inhibits tumor growth in preclinical models of cancer, *Clin. Cancer Res.*, 2012, **18**, 758–770.

11 Q. Wang, Y. Song, S. Yuan, Y. Zhu, W. Wang and L. Chu, Prodrug activation by 4,4′-bipyridine-mediated aromatic nitro reduction, *Nat. Commun.*, 2024, **15**, 8643.

12 C. Ward, S. P. Langdon, P. Mullen, A. L. Harris, D. J. Harrison, C. T. Supuran and I. H. Kunkler, New strategies for targeting the hypoxic tumour microenvironment in breast cancer, *Cancer Treat. Rev.*, 2013, **39**, 171–179.

13 K. Ameri, R. Luong, H. Zhang, A. A. Powell, K. D. Montgomery, I. Espinosa, D. M. Bouley, A. L. Harris and S. S. Jeffrey, Circulating tumour cells demonstrate an altered response to hypoxia and an aggressive phenotype, *Br. J. Cancer*, 2010, **102**, 561–569.

14 L. J. Yu, J. Matias, D. A. Scudiero, K. M. Hite, A. Monks, E. A. Sausville and D. J. Waxman, P450 enzyme expression patterns in the NCI human tumor cell line panel, *Drug Metab. Dispos.*, 2001, **29**, 304–312.

15 Y. Wang, J. P. Gray, V. Mishin, D. E. Heck, D. L. Laskin and J. D. Laskin, Distinct roles of cytochrome P450 reductase in mitomycin C redox cycling and cytotoxicity, *Mol. Cancer Ther.*, 2010, **9**, 1852–1863.

16 M. A. Naylor and P. Thomson, Recent advances in bioreductive drug targeting, *Mini-Rev. Med. Chem.*, 2001, **1**, 17–29.

17 P. Reigan, P. N. Edwards, A. Gbaj, C. Cole, S. T. Barry, K. M. Page, S. E. Ashton, R. W. Luke, K. T. Douglas, I. J. Stratford, M. Jaffar, R. A. Bryce and S. Freeman, Aminoimidazolylmethyluracil analogues as potent inhibitors of thymidine phosphorylase and their bioreductive nitroimidazolyl prodrugs, *J. Med. Chem.*, 2005, **48**, 392–402.

18 N. Baran and M. Konopleva, Molecular Pathways: Hypoxia-Activated Prodrugs in Cancer Therapy, *Clin. Cancer Res.*, 2017, **23**, 2382–2390.

19 F. Meng, J. W. Evans, D. Bhupathi, M. Banica, L. Lan, G. Lorente, J. X. Duan, X. Cai, A. M. Mowday, C. P. Guise, A. Maroz, R. F. Anderson, A. V. Patterson, G. C. Stachelek, P. M. Glazer, M. D. Matteucci and C. P. Hart, Molecular and cellular pharmacology of the hypoxia-activated prodrug TH-302, *Mol. Cancer Ther.*, 2012, **11**, 740–751.

20 K. Hendricksen, D. Gleason, J. M. Young, D. Saltzstein, A. Gershman, S. Lerner and J. A. Witjes, Safety and side effects of immediate instillation of apaziquone following transurethral resection in patients with nonmuscle invasive bladder cancer, *J. Urol.*, 2008, **180**, 116–120.

21 M. J. McKeage, Y. Gu, W. R. Wilson, A. Hill, K. Amies, T. J. Melink and M. B. Jameson, A phase I trial of PR-104, a pre-prodrug of the bioreductive prodrug PR-104A, given weekly to solid tumour patients, *BMC Cancer*, 2011, **11**, 432.

22 M. P. Saunders, A. V. Patterson, E. C. Chinje, A. L. Harris and I. J. Stratford, NADPH:cytochrome c (P450) reductase activates tirapazamine (SR4233) to restore hypoxic and oxic cytotoxicity in an aerobic resistant derivative of the A549 lung cancer cell line, *Br. J. Cancer*, 2000, **82**, 651–656.

23 B. G. Siim, F. B. Pruijn, J. R. Sturman, A. Hogg, M. P. Hay, J. M. Brown and W. R. Wilson, Selective potentiation of the hypoxic cytotoxicity of tirapazamine by its 1-N-oxide metabolite SR 4317, *Cancer Res.*, 2004, **64**, 736–742.

24 A. Yaromina, L. Koi, L. Schuitmaker, A. M. M. A. van der Wiel, L. J. Dubois, M. Krause and P. Lambin, Overcoming radioresistance with the hypoxia-activated prodrug CP-506: A pre-clinical study of local tumour control probability, *Radiother. Oncol.*, 2023, **186**, 109738.

25 M. R. Albertella, P. M. Loadman, P. H. Jones, R. M. Phillips, R. Rampling, N. Burnet, C. Alcock, A. Anthoney, E. Vjaters, C. R. Dunk, P. A. Harris, A. Wong, A. S. Lalani and C. J. Twelves, Hypoxia-selective targeting by the bioreductive prodrug AQ4N in patients with solid tumors: results of a phase I study, *Clin. Cancer Res.*, 2008, **14**, 1096–1104.

26 C. P. Guise, A. M. Mowday, A. Ashoorzadeh, R. Yuan, W. H. Lin, D. H. Wu, J. B. Smaill, A. V. Patterson and K. Ding, Bioreductive prodrugs as cancer therapeutics: targeting tumor hypoxia, *Chin. J. Cancer*, 2014, **33**, 80–86.

27 W. A. Denny, Nitroaromatic Hypoxia-Activated Prodrugs for Cancer Therapy, *Pharmaceuticals*, 2022, **15**, 187.

28 C. Braga, M. Ferreira-Silva, M. L. Corvo, R. Moreira, A. R. Fernandes, J. Vaz and M. J. Perry, Nitroaromatic-based triazene prodrugs to target the hypoxic microenvironment in glioblastoma, *RSC Med. Chem.*, 2025, **16**, 1350–1362.

29 A. Sharma, J. F. Arambula, S. Koo, R. Kumar, H. Singh, J. L. Sessler and J. S. Kim, Hypoxia-targeted drug delivery, *Chem. Soc. Rev.*, 2019, **48**, 771–813.

30 S. Karan, M. Y. Cho, H. Lee, H. M. Kim, H. S. Park, E. H. Han, J. L. Sessler and K. S. Hong, Hypoxia-Directed and Self-Immolative Theranostic Agent: Imaging and Treatment of Cancer and Bacterial Infections, *J. Med. Chem.*, 2023, **66**, 14175–14187.

31 B. D. Dickson, W. W. Wong, W. R. Wilson and M. P. Hay, Studies Towards Hypoxia-Activated Prodrugs of PARP Inhibitors, *Molecules*, 2019, **24**, 1559.
32 Y. Ye, Q. Hu, H. Chen, K. Liang, Y. Yuan, Y. Xiang, H. Ruan, Z. Zhang, A. Song, H. Zhang, L. Liu, L. Diao, Y. Lou, B. Zhou, L. Wang, S. Zhou, J. Gao, E. Jonasch, S. H. Lin, Y. Xia, C. Lin, L. Yang, G. B. Mills, H. Liang and L. Han, Characterization of Hypoxia-associated Molecular Features to Aid Hypoxia-Targeted Therapy, *Nat. Metab.*, 2019, **1**, 431–444.
33 G. R. Pettit, S. B. Singh, M. R. Boyd, E. Hamel, R. K. Pettit, J. M. Schmidt and F. Hogan, Antineoplastic agents. 291. Isolation and synthesis of combretastatins A-4, A-5, and A-6(1a), *J. Med. Chem.*, 1995, **38**, 1666–1672.
34 G. R. Pettit, S. B. Singh, M. L. Niven, E. Hamel and J. M. Schmidt, Antineoplastic agents 124. Isolation, structure, and synthesis of combretastatin-A-1 and combretasatin-B-1, potent new inhibitors of microtubule assembly, derived from combretum-caffrum, *J. Nat. Prod.*, 1987, **50**, 119–131.
35 M. Sriram, J. J. Hall, N. C. Grohmann, T. E. Strecker, T. Wootton, A. Franken, M. L. Trawick and K. G. Pinney, Design, synthesis and biological evaluation of dihydronaphthalene and benzosuberene analogs of the combretastatins as inhibitors of tubulin polymerization in cancer chemotherapy, *Bioorg. Med. Chem. Lett.*, 2008, **16**, 8161–8171.
36 R. P. Tanpure, C. S. George, T. E. Strecker, L. Devkota, J. K. Tidmore, C. M. Lin, C. A. Herdman, M. T. MacDonough, M. Sriram, D. J. Chaplin, M. L. Trawick and K. G. Pinney, Synthesis of structurally diverse benzosuberene analogues and their biological evaluation as anti-cancer agents, *Bioorg. Med. Chem. Lett.*, 2013, **21**, 8019–8032.
37 C. A. Herdman, L. Devkota, C. M. Lin, H. C. Niu, T. E. Strecker, R. Lopez, L. Liu, C. S. George, R. P. Tanpure, E. Hamel, D. J. Chaplin, R. P. Mason, M. L. Trawick and K. G. Pinney, Structural interrogation of benzosuberene-based inhibitors of tubulin polymerization, *Bioorg. Med. Chem. Lett.*, 2015, **23**, 7497–7520.
38 M. B. Hadimani, M. T. MacDonough, A. Ghatak, T. E. Strecker, R. Lopez, M. Sriram, B. L. Nguyen, J. J. Hall, R. J. Kessler, A. R. Shirali, L. Liu, C. M. Garner, G. R. Pettit, E. Hamel, D. J. Chaplin, R. P. Mason, M. L. Trawick and K. G. Pinney, Synthesis of a 2-Aryl-3-aroyl Indole Salt (OXi8007) Resembling Combretastatin A-4 with Application as a Vascular Disrupting Agent, *J. Nat. Prod.*, 2013, **76**, 1668–1678.
39 M. T. MacDonough, T. E. Strecker, E. Hamel, J. J. Hall, D. J. Chaplin, M. L. Trawick and K. G. Pinney, Synthesis and biological evaluation of indole-based, anti-cancer agents inspired by the vascular disrupting agent 2-(3′-hydroxy-4′-methoxyphenyl)-3-(3″,4″,5″-trimethoxybenzoyl)-6-methoxyindole (OXi8006), *Bioorg. Med. Chem. Lett.*, 2013, **21**, 6831–6843.
40 E. Hamel and C. M. Lin, Stabilization of the colchicine-binding activity of tubulin by organic acids, *Biochim. Biophys. Acta*, 1981, **675**, 226–231.
41 J. K. Batra, G. J. Kang, L. Jurd and E. Hamel, Methylenedioxy-benzopyran analogs of podophyllotoxin, a new synthetic class of antimitotic agents that inhibit tubulin polymerization, *Biochem. Pharmacol.*, 1988, **37**, 2595–2602.
42 Z. Shah, U. F. Gohar, I. Jamshed, A. Mushtaq, H. Mukhtar, M. Zia-Ui-Haq, S. I. Toma, R. Manea, M. Moga and B. Popovici, Podophyllotoxin: History, Recent Advances and Future Prospects, *Biomolecules*, 2021, **11**, 603.
43 P. Thomson, M. A. Naylor, S. A. Everett, M. R. Stratford, G. Lewis, S. Hill, K. B. Patel, P. Wardman and P. D. Davis, Synthesis and biological properties of bioreductively targeted nitrothienyl prodrugs of combretastatin A-4, *Mol. Cancer Ther.*, 2006, **5**, 2886–2894.
44 R. P. Tanpure, C. S. George, M. Sriram, T. E. Strecker, J. K. Tidmore, E. Hamel, A. K. Charlton-Sevcik, D. J. Chaplin, M. L. Trawick and K. G. Pinney, An amino-benzosuberene analogue that inhibits tubulin assembly and demonstrates remarkable cytotoxicity, *MedChemComm*, 2012, **3**, 720–724.
45 C. J. Maguire, Z. Chen, V. P. Mocharla, M. Sriram, T. E. Strecker, E. Hamel, H. Zhou, R. Lopez, Y. Wang, R. P. Mason, D. J. Chaplin, M. L. Trawick and K. G. Pinney, Synthesis of dihydronaphthalene analogues inspired by combretastatin A-4 and their biological evaluation as anticancer agents, *MedChemComm*, 2018, **9**, 1649–1662.
46 L. Devkota, C. M. Lin, T. E. Strecker, Y. F. Wang, J. K. Tidmore, Z. Chen, R. Guddneppanavar, C. J. Jelinek, R. Lopez, L. Liu, E. Hamel, R. P. Mason, D. J. Chaplin, M. L. Trawick and K. G. Pinney, Design, synthesis, and biological evaluation of water-soluble amino acid prodrug conjugates derived from combretastatin, dihydronaphthalene, and benzosuberene-based parent vascular disrupting agents, *Bioorg. Med. Chem. Lett.*, 2016, **24**, 938–956.
47 H. Niu, T. E. Strecker, J. L. Gerberich, J. W. Campbell, 3rd, D. Saha, D. Mondal, E. Hamel, D. J. Chaplin, R. P. Mason, M. L. Trawick and K. G. Pinney, Structure Guided Design, Synthesis, and Biological Evaluation of Novel Benzosuberene Analogues as Inhibitors of Tubulin Polymerization, *J. Med. Chem.*, 2019, **62**, 5594–5615.
48 J. M. VanNatta, H. Niu, G. J. Carlson and K. G. Pinney, Application of Chlorosulfonyl Isocyanate (CSI) in the Synthesis of Fused Tetracyclic Ketone Ring Systems, *J. Org. Chem.*, 2024, **89**, 15636–15651.
49 R. Grisham, B. Ky, K. S. Tewari, D. J. Chaplin and J. Walker, Clinical trial experience with CA4P anticancer therapy: focus on efficacy, cardiovascular adverse events, and hypertension management, *Gynecol. Oncol. Res. Pract.*, 2018, **5**, 1.
50 R. P. Mason, D. Zhao, L. Liu, M. L. Trawick and K. G. Pinney, A Perspective on Vascular Disrupting Agents that Interact with Tubulin: Preclinical Tumor Imaging and Biological Assessment, *Integr. Biol.*, 2011, **3**, 375–387.
51 D. J. Chaplin, M. R. Horsman and D. W. Siemann, Current development status of small-molecule vascular disrupting agents, *Curr. Opin. Invest. Drugs*, 2006, **7**, 522–528.
52 D. Zhao, E. Richer, P. P. Antich and R. P. Mason, Antivascular effects of combretastatin A4 phosphate in breast cancer xenograft assessed using dynamic bioluminescence imaging

(BLI) and confirmed by magnetic resonance imaging (MRI), *FASEB J.*, 2008, **22**, 2445–2451.

53 G. R. Pettit, B. Toki, D. L. Herald, P. Verdier-Pinard, M. R. Boyd, E. Hamel and R. K. Pettit, Antineoplastic agents. 379. Synthesis of phenstatin phosphate, *J. Med. Chem.*, 1998, **41**, 1688–1695.

54 B. A. Winn, Z. Shi, G. J. Carlson, Y. F. Wang, B. L. Nguyen, E. M. Kelly, R. D. Ross, E. Hamel, D. J. Chaplin, M. L. Trawick and K. G. Pinney, Bioreductively activatable prodrug conjugates of phenstatin designed to target tumor hypoxia, *Bioorg. Med. Chem. Lett.*, 2017, **27**, 636–641.

55 B. A. Winn, L. Devkota, B. Kuch, M. T. MacDonough, T. E. Strecker, Y. Wang, Z. Shi, J. L. Gerberich, D. Mondal, A. J. Ramirez, E. Hamel, D. J. Chaplin, P. Davis, R. P. Mason, M. L. Trawick and K. G. Pinney, Bioreductively Activatable Prodrug Conjugates of Combretastatin A-1 and Combretastatin A-4 as Anticancer Agents Targeted toward Tumor-Associated Hypoxia, *J. Nat. Prod.*, 2020, **83**, 937–954.

56 J. M. VanNatta, G. J. Carlson, H. Niu, R. Bai, H. I. Wanniarachchi, R. Schuetze, M. L. Trawick, E. Hamel, R. P. Mason and K. G. Pinney, Benzosuberene and Tetracyclic Analogues as Colchicine Site Inhibitors of Tubulin Polymerization, *ACS Med. Chem. Lett.*, 2025, **16**, 1098–1107.

57 W. Ren, Y. Deng, J. D. Ward, R. Vairin, R. Bai, H. I. Wanniarachchi, K. B. Hamal, P. E. Tankoano, C. S. Tamminga, L. M. A. Bueno, E. Hamel, R. P. Mason, M. L. Trawick and K. G. Pinney, Synthesis and biological evaluation of structurally diverse 6-aryl-3-aroyl-indole analogues as inhibitors of tubulin polymerization, *Eur. J. Med. Chem.*, 2024, **263**, 115794.

58 R. Vairin, C. Tamminga, Z. Shi, C. Borchardt, J. Jambulapati, R. Bai, H. Wanniarachchi, L. Bueno, E. Hamel, R. P. Mason, M. L. Trawick and K. G. Pinney, Design, synthesis and biological evaluation of 2-phenyl indole analogues of OXi8006 as colchicine site inhibitors of tubulin polymerization and vascular disrupting agents, *Bioorg. Med. Chem.*, 2024, 117981.

59 L. J. O'Connor, C. Cazares-Korner, J. Saha, C. N. G. Evans, M. R. L. Stratford, E. M. Hammond and S. J. Conway, Efficient synthesis of 2-nitroimidazole derivatives and the bioreductive clinical candidate Evofosfamide (TH-302), *Org. Chem. Front.*, 2015, **2**, 1026–1029.

60 L. J. O'Connor, C. Cazares-Korner, J. Saha, C. N. Evans, M. R. Stratford, E. M. Hammond and S. J. Conway, Design, synthesis and evaluation of molecularly targeted hypoxia-activated prodrugs, *Nat. Protoc.*, 2016, **11**, 781–794.

61 D. Mondal, H. Niu and K. G. Pinney, Efficient Synthetic Methodology for the Construction of Dihydronaphthalene and Benzosuberene Molecular Frameworks, *Tetrahedron Lett.*, 2019, **60**, 397–401.

62 K. C. Swamy, N. N. Kumar, E. Balaraman and K. V. Kumar, Mitsunobu and related reactions: advances and applications, *Chem. Rev.*, 2009, **109**, 2551–2651.

63 K. Nepali, H. Y. Lee and J. P. Liou, Nitro-Group-Containing Drugs, *J. Med. Chem.*, 2019, **62**, 2851–2893.

64 S. T. Abreu, L. G. V. Gelves, E. J. Barreiro and L. M. Lima, Revisiting Nitroaromatic Drugs: Mechanisms of Bioactivation, Metabolism and Toxicity and Methods to Synthesize Nitroaromatic Fragments, *J. Braz. Chem. Soc.*, 2024, **35**(10), e-20240071.

65 L. S. Ryan, J. Gerberich, J. Cao, W. An, B. A. Jenkins, R. P. Mason and A. R. Lippert, Kinetics-Based Measurement of Hypoxia in Living Cells and Animals Using an Acetoxymethyl Ester Chemiluminescent Probe, *ACS Sens.*, 2019, **4**, 1391–1398.

66 E. E. Graves, M. Vilalta, I. K. Cecic, J. T. Erler, P. T. Tran, D. Felsher, L. Sayles, A. Sweet-Cordero, Q. T. Le and A. J. Giaccia, Hypoxia in Models of Lung Cancer: Implications for Targeted Therapeutics, *Clin. Cancer Res.*, 2010, **16**, 4843–4852.

67 L. D. Skarsgard, D. K. Acheson, A. Vinczan, B. G. Wouters, B. E. Heinrichs, D. A. Loblaw, A. I. Minchinton and D. J. Chaplin, Cytotoxic effect of RB 6145 in human tumour cell lines: dependence on hypoxia, extra- and intracellular pH and drug uptake, *Br. J. Cancer*, 1995, **72**, 1479–1486.

68 F. W. Hunter, R. J. Young, Z. Shalev, R. N. Vellanki, J. Wang, Y. Gu, N. Joshi, S. Sreebhavan, I. Weinreb, D. P. Goldstein, J. Moffat, T. Ketela, K. R. Brown, M. Koritzinsky, B. Solomon, D. Rischin, W. R. Wilson and B. G. Wouters, Identification of P450 Oxidoreductase as a Major Determinant of Sensitivity to Hypoxia-Activated Prodrugs, *Cancer Res.*, 2015, **75**, 4211–4223.

69 K. J. Nytko, I. Grgic, S. Bender, J. Ott, M. Guckenberger, O. Riesterer and M. Pruschy, The hypoxia-activated prodrug evofosfamide in combination with multiple regimens of radiotherapy, *Oncotarget*, 2017, **8**, 23702–23712.

70 L. Liu, D. O'Kelly, R. Schuetze, G. Carlson, H. Zhou, M. L. Trawick, K. G. Pinney and R. P. Mason, Non-Invasive Evaluation of Acute Effects of Tubulin Binding Agents: A Review of Imaging Vascular Disruption in Tumors, *Molecules*, 2021, **26**, 2551.

71 K. Tao, M. Fang, J. Alroy and G. G. Sahagian, Imagable 4T1 model for the study of late stage breast cancer, *BMC Cancer*, 2008, **8**, 228.

72 Y. Zhang, H. Hong, T. R. Nayak, H. F. Valdovinos, D. V. Myklejord, C. P. Theuer, T. E. Barnhart and W. Cai, Imaging tumor angiogenesis in breast cancer experimental lung metastasis with positron emission tomography, near-infrared fluorescence, and bioluminescence, *Angiogenesis*, 2013, **16**, 663–674.

73 Y. Guo, H. Wang, J. L. Gerberich, S. O. Odutola, A. K. Charlton-Sevcik, M. Li, R. P. Tanpure, J. K. Tidmore, M. L. Trawick, K. G. Pinney, R. P. Mason and L. Liu, Imaging-Guided Evaluation of the Novel Small-Molecule Benzosuberene Tubulin-Binding Agent KGP265 as a Potential Therapeutic Agent for Cancer Treatment, *Cancers*, 2021, **13**, 4769.

74 L. Liu, R. Schuetze, J. L. Gerberich, R. Lopez, S. O. Odutola, R. P. Tanpure, A. K. Charlton-Sevcik, J. K. Tidmore, E. A. Taylor, P. Kapur, H. Hammers, M. L. Trawick, K. G. Pinney and R. P. Mason, Demonstrating Tumor Vascular Disrupting Activity of the Small-Molecule Dihydronaphthalene Tubulin-Binding Agent OXi6196 as a Potential Therapeutic for Cancer Treatment, *Cancers*, 2022, **14**, 4208.

75 H. I. Wanniarachchi, R. Schuetze, Y. Deng, K. B. Hamal, C. I. Pavlich, P. E. O. Tankoano, C. Tamminga, H. Hammers, P. Kapur, L. M. A. Bueno, R. Rayas, T. Wang, L. Liu, M. L. Trawick, K. G. Pinney and R. P. Mason, Evaluating Therapeutic Efficacy of the Vascular Disrupting Agent OXi8007 Against Kidney Cancer in Mice, *Cancers*, 2025, **17**, 771.

76 B. A. Pulaski and S. Ostrand-Rosenberg, Reduction of established spontaneous mammary carcinoma metastases following immunotherapy with major histocompatibility complex class II and B7.1 cell-based tumor vaccines, *Cancer Res.*, 1998, **58**, 1486–1493.

77 M. Jaffar, R. M. Phillips, K. J. Williams, I. Mrema, C. Cole, N. S. Wind, T. H. Ward, I. J. Stratford and A. V. Patterson, 3-substituted-5-aziridinyl-1-methylindole-4,7-diones as NQO1-directed antitumour agents: mechanism of activation and cytotoxicity in vitro, *Biochem. Pharmacol.*, 2003, **66**, 1199–1206.

78 R. Siles, J. F. Ackley, M. B. Hadimani, J. J. Hall, B. E. Mugabe, R. Guddneppanavar, K. A. Monk, J. C. Chapuis, G. R. Pettit, D. J. Chaplin, K. Edvardsen, M. L. Trawick, C. M. Garner and K. G. Pinney, Combretastatin dinitrogen-substituted stilbene analogues as tubulin-binding and vascular-disrupting agents, *J. Nat. Prod.*, 2008, **71**, 313–320.

79 A. Monks, D. Scudiero, P. Skehan, R. Shoemaker, K. Paull, D. Vistica, C. Hose, J. Langley, P. Cronise and A. Vaigro-Wolff, *et al.*, Feasibility of a high-flux anticancer drug screen using a diverse panel of cultured human tumor cell lines, *J. Natl. Cancer Inst.*, 1991, **83**, 757–766.

80 V. Vichai and K. Kirtikara, Sulforhodamine B colorimetric assay for cytotoxicity screening, *Nat. Protoc.*, 2006, **1**, 1112–1116.

81 W. Voigt, Sulforhodamine B assay and chemosensitivity, *Methods Mol. Med.*, 2005, **110**, 39–48.

82 K. Blaszczak-Swiatkiewicz and E. Mikiciuk-Olasik, Biological evaluation of the activity of some benzimidazole-4,7-dione derivatives, *Molecules*, 2014, **19**, 15361–15373.

83 E. Hamel, Evaluation of antimitotic agents by quantitative comparisons of their effects on the polymerization of purified tubulin, *Cell Biochem. Biophys.*, 2003, **38**, 1–22.

84 F. P. Guengerich, M. V. Martin, C. D. Sohl and Q. Cheng, Measurement of cytochrome P450 and NADPH-cytochrome P450 reductase, *Nat. Protoc.*, 2009, **4**, 1245–1251.

85 (*a*) Z. Shi, Small-Molecule Inhibitors of Tubulin Polymerization as Vascular Disrupting Agents and Prodrugs Targeting Tumor-Associated Hypoxia, *Ph.D. Dissertation*, Baylor University, 2018; (*b*) B. A. Winn, Synthesis, Characterization, and Biological Evaluation of Bioreductively Activatable Prodrug Conjugates (BAPCs) of Phenstatin, KGP18, OXi6196, Combretastatin A-1, and Combretastatin A-4, *Ph.D. Dissertation*, Baylor University, 2017; (*c*) M. T. MacDonough, The Design, Synthesis, and Biological Evaluation of Indole-based Anticancer Agents, *Ph.D. Dissertation*, Baylor University, 2013; (*d*) C. S. George, Targeting the Tumor Microenvironment Through the Design and Synthesis of Potent, Small-Molecule, Anticancer Agents, *Ph.D. Dissertation*, Baylor University, 2012; (*e*) C. J. Maguire, Design, Synthesis, and Biological Evaluation of Dihydronaphthalene and Chalcone-based Anticancer Agents Inspired by the Natural Product Combretastatin A-4, *Ph.D. Dissertation*, Baylor University, 2019; (*f*) J. W. Ford, The Development of Prodrug Strategies for the Targeted Delivery of Dihydronaphthalene and Benzosuberene Inhibitors of Tubulin Polymerization, *Ph.D. Dissertation*, Baylor University, 2021.